Tectonophysics 710–711 (2017) 108–126

Contents lists available at ScienceDirect

Tectonophysics

journal homepage: www.elsevier.com/locate/tecto

From stretching to mantle exhumation in a triangular backarc basin (Vavilov basin, Tyrrhenian Sea, Western Mediterranean)

A. Milia [a,*], M.M. Torrente [b], M. Tesauro [c]

[a] IAMC, CNR, Calata Porta di Massa, Porto di Napoli, I-80100 Naples, Italy
[b] DST, Università del Sannio, Via dei Mulini 59/A, I-82100 Benevento, Italy
[c] Utrecht University, Budapestlaan, 6, 3584 CD Utrecht, Netherlands

ARTICLE INFO

Article history:
Received 29 January 2016
Received in revised form 3 October 2016
Accepted 18 October 2016
Available online 24 October 2016

Keywords:
Triangular backarc basins
Tectono-stratigraphy
Extensional modes
Vavilov basin
Tyrrhenian Sea

ABSTRACT

In this study, we describe the mode of extension of the Vavilov, a fossil backarc basin, triangle-shaped (approximately 240 km-wide and 200 km-long), located between Sardinia margin to the west and Campania margin to the east. We combine the analysis of recent geophysical and geological data, in order to investigate the relationship between the crustal/sedimentary structure and the tectonic evolution of both apex and bathyal parts of the basin. With this aim, we interpret a large data set of multichannel seismic reflection profiles and several well logs. We observe that the apex basin corresponds to a sediment-balanced basin, with a sedimentary infill recording the episodes of basin evolution. In contrast, the distal basin corresponds to an underfilled basin, characterized by localized volcanic activity and a thin sedimentary succession that covers the exhumed mantle. The basin architecture reveals the occurrence of rift and supradetachment basins in the Vavilov rift zone. We find that the rifting of the Vavilov triangular basin was synchronous from the apex to distal regions around a single Euler pole located in Latium, between 5.1 and 1.8 Ma. The kinematic evolution of the Vavilov basin occurred in two stages: initial pure shear mode (5.1–4.0 Ma) that produced high-angle normal faults and syn-sedimentary wedges, followed by simple shear mode (4.0–1.8 Ma) that caused supradetachment basins filled by a Transgressive-Regressive succession that documents high subsidence rates (1.22 mm/y) in the apex region. The final stage of extension in the distal region led to: (i) complete embrittlement of the crust; (ii) direct continuation of crustal faults to upper mantle depth; (iii) serpentinization and mantle exhumation. Based on constraints on the present-day crustal structure of the Vavilov basin, we obtain a stretching value ($\beta = 3.5$) and extension rates (3 cm/y) in the bathyal zone analogous to those reported for magma-poor rifted margins.

1. Introduction

In recent decades many studies have been carried out on rift formation, in order to understand causes and modes of whole lithospheric extension (e.g., Coward et al., 1987; Keen, 1987; Ziegler, 1992; Ruppel, 1995; Corti et al., 2003; Ziegler and Cloetingh, 2004). Data recorded from a large number of extensional regions worldwide indicate that rifting is a polyphasic process, since rift activity migrates and the mode of extension (symmetric to asymmetric pattern) changes through time (e.g., Whitmarsh et al., 2001; Reston and Pérez-Gussinyé, 2007; Reston, 2009; Espur et al., 2012; Cloetingh et al., 2013). A critical step to reconstruct the evolution of a rift zone is the stratigraphic analysis of ancient and active rift basins. This analysis indicates that development of normal faults, their physiographic expressions, and variations in fault slip rates are the major factors influencing the spatial distribution and architecture of depositional systems adjacent to the fault zones (e.g., Dart et al., 1994; Gawthorpe and Leeder, 2000). Extensional sedimentary basins can be classified in terms of stratigraphy, age of formation, basin architecture, and bounding fault's geometry. Friedman and Burbank (1995) proposed that continental extensional tectonism has two end-members styles: rift settings and highly extended terrains, resulting in high-angle rift basins and supradetachment basins, respectively. The evolution from rift systems to supradetachment basins depends on different factors, such as crustal thickness, thermal state of the lithosphere, and tectonic environment. Temporal changes of these parameters influence the basin structure. In particular, supradetachment basins are characterized by thick or over thickened, recently active lithosphere in a backarc setting (e.g., Coney, 1987).

Extensional basins have been studied and classified using 2D geological sections (e.g., McKenzie, 1978; Bally et al., 1981; Wernicke, 1985; Lister et al., 1986; McClay and Ellis, 1987) and thus also modelled prevalently in 2D (e.g., Wernicke and Axen, 1988; Whitmarsh et al., 2001; Harris et al., 2002; Corti et al., 2003; Kapp et al., 2008; Brune et al., 2014; Platt et al., 2015). However, the complete process of continental

* Corresponding author.
E-mail addresses: alfonsa.milia@iamc.cnr.it (A. Milia), torrente@unisannio.it (M.M. Torrente), m.tesauro@uu.nl (M. Tesauro).

http://dx.doi.org/10.1016/j.tecto.2016.10.017
0040-1951/

break-up can be understood only through detailed 3D studies of rift evolution at varying stretching factors (Reston and Pérez-Gussinyé, 2007). Up to now, only few studies use a three-dimensional approach to investigate the evolution of rift basins (Martin, 1984, 2006; Schellart et al., 2003; Lavier and Manatschal, 2006; Sokoutis et al., 2007; Smit et al., 2010).

Natural examples and models have described the modes of extension from stretching to continental break-up and oceanization in magma-poor rifted margins (e.g., Whitmarsh et al., 2001). Even if these types of extension have been observed in the present and fossil Atlantic basins (Manatschal, 2004; Péron-Pinvidic et al., 2007; Espur et al., 2012; Masini et al., 2012), exhumed mantle or hyper-extended crust are also typical features of backarc basins (Taylor, 1995), which can become parts of orogenic belts (Saintot et al., 2003; Butler et al., 2006; Stephenson et al., 2006; Roure et al., 2012).

According to Whitmarsh et al. (2001), the evolution of a rift area occurs with two consecutive modes of continental extension: pure shear and simple shear. The pure shear mode is characterized by high differential subsidence of half-grabens and lithospheric necking. The simple shear mode is instead characterized by lithospheric detachment faulting, strong subsidence, deposition of sub-horizontal strata, and final exhumation of serpentinized upper mantle, uprising from a depth <10 km along a downward-concave fault.

Although models of rifts have been largely developed for Atlantic type margins, the Vavilov backarc basin in the Tyrrhenian Sea is the ideal place to study different stages of rifting until mantle exhumation. The Tyrrhenian Sea (Fig. 1) is the youngest backarc basin of the Western Mediterranean (e.g., Dewey et al., 1989). Crustal thinning and opening of sedimentary basins in the Tyrrhenian Sea have been documented since the start of Deep Sea Drilling Project (DSDP) and Ocean Drilling Program (ODP) (Hsu et al., 1978; Kastens et al., 1987; Spadini et al., 1995).Within this geological framework, the Vavilov basin represents a perfectly preserved fossil triangular basin, where the extensional processes reached the mantle exhumation stage during the Pliocene (Mascle and Rehault, 1990; Milia et al., 2013) and moved eastwards in the Quaternary (Milia and Torrente, 2015a).

In this study, we interpret seismic reflection profiles and wells data, in order to reconstruct the architecture and timing of rifting of the Vavilov basin. Our results show rift and supradetachment basins in the Vavilov rift zone and, for the first time, the kinematics of the entire triangular basin (from apex to distal zones). Furthermore, we compare the development of the Vavilov basin with two evolutionary models of triangular basins: a) the plate tectonic rift model, featuring a synchronous opening across the whole basin, from apex to the distal part around a rotation pole (e.g., Martin, 1984, 2006); b) the propagating rift model, characterized by an extension migration from the distal to the apex of the basin (Lavier and Manatschal, 2006). On the basis of this comparison and the crustal structure of the Vavilov basin, we propose a model of tectonic evolution of the study region.

2. Geologic framework

The Tyrrhenian Sea is a Neogene-Quaternary triangular land-locked extensional basin that formed at the rear of the Neogene Apennine thrust belt (e.g., Kastens and Mascle, 1990; Patacca et al., 1990). Its backarc evolution has mainly been attributed to the rollback toward the south-east of the subducting Ionian plate (e.g., Malinverno and Ryan, 1986, Cavinato and De Celles, 1999; Faccenna et al., 1996; Rosenbaum and Lister, 2004). The central abyssal plain (depth > 3000 m) of the Tyrrhenian Sea is characterized by a thin crust (from 15 to <10 km) and lithosphere (~30 km) (Panza, 1984; Nicolich, 1989; Cassinis et al., 2003), high heat flow values (Della Vedova et al., 2001), and a large positive Bouger gravity anomaly (Mongelli et al., 1975). Rocks of the different geological domains, outcropping onland and mainly formed during the Alpine orogenic cycle (e.g., Sartori, 2005), have been dredged in the Tyrrhenian area. They represent fragments of the European continent (Corsica and Sardinia), Tethyan ophiolites, Calabria crystalline terrane, and Apenninic-Maghrebian chain.

The Tyrrhenian Basin can be divided into northern and southern sectors characterized by different extension values. The northern Tyrrhenian Sea started to form in the lower Miocene as a polyphase rift, displaying a trend of faults convergent toward the North. This basin has a relatively low value of stretching (e.g., Cornamusini et al., 2002; Pascucci, 2002), constrained by crustal thickness that ranges between 25 and 20 km (Nicolich, 1989). In contrast, the Southern Tyrrhenian Sea (Fig. 1) is a middle Miocene–Quaternary polyphase rift with several fault trends, which includes the Vavilov basin. The stretching factor of the Southern Tyrrhenian Sea is relatively high. The Vavilov basin displays a detachment fault cutting the whole crust, which is responsible for the exhumation of serpentinized peridotites of the mantle (Kastens et al., 1987; Mascle and Rehault, 1990; Milia et al., 2013).

The Vavilov rift zone is flanked in the west by the Cornaglia basin and in the east by the Campania margin (Fig. 1). The Cornaglia basin formed during the upper Miocene on the Sardinia continental margin (e.g., Alvarez et al., 1974; Sartori, 1990, 2003; Spadini et al., 1995; Rosenbaum and Lister, 2004; Milia and Torrente, 2014) and was displaced by high-angle normal faults trending N-S. The associated synrift sedimentary wedges correspond to thick Tortonian-Messinian clastic deposits, conformably overlain by thin post-rift early Pliocene deposits (MPL1; Fig. 1). Different ages for the rifting of the Vavilov basin have been proposed: upper Tortonian-Messinian (Mascle and Rehault, 1990), upper Messinian (Sartori et al., 2004) and late Messinian-early Pliocene (Sartori, 1990). Extensional processes developed on the Campania margin over the last 1.3 Ma (Torrente et al., 2010; Milia and Torrente, 2015a). The stratigraphy of the Vavilov bathyal zone is recorded by the ODP sites 655, 651 and DSDP site 373 (Fig. 1). Site 655, located on the crest of the Gortani Ridge, encountered 80 m of sediments, middle Pliocene (MPL4/NN15)-Quaternary in age, which are lying above and interlayered by MORB basalts (Kastens et al., 1987). At Site 651 (Kastens et al., 1987) 388 m of marine sediment (MPL6/NN18-Quaternary) overlain 39 m thick of undated dolostones. The basement section is formed by three units: basalts, transition zone, and highly serpentinized peridotites, showing a tectonic foliation. The basalts, dated 2.4 Ma (Robin et al., 1987), present carbonate veins, which decrease downhole, plus carbonate-opal-cemented basaltic breccias. The 58 m-thick transition zone comprises two subunits: (i) highly altered peridotites, dolerites, dolomitic chalk, alkali feldspar-rich leucocratic rocks, carbonate-cemented basaltic breccias, a very coarse sand to fine gravel graded layer, and a few rounded loose pebbles of metadolerite. The deepest occurrence of planktonic foraminifers is in a dolomitic breccia, tentatively dated early Pliocene; (ii) a lower thin layer of basalts and basaltic breccias, which could represent tectonic and/or talus breccias, cemented by carbonate sediment filling and carbonate precipitation from circulating seawater. At Site 373, 187 m of basaltic breccias and flows, dated 7–4.4 Ma (Savelli and Lipparini, 1978), are covered by a 270 m thick Lower Pliocene (MPL3/NN14)-Pleistocene succession (Hsu et al., 1978).

The Latium Apennines fold-and-thrust belt is composed of two tectonic units: the Liguride thrust sheet overlying the Carbonate thrust sheet. The Liguride unit, composed of Cretaceous-Miocene clays, marls and sands, was deposited on oceanic or thinned continental crust and is encountered at depth ranging between ~250 and ~1550 m by onshore boreholes near Anzio (Fig. 2). The Trias-Miocene Carbonate unit was deposited on the continental crust of Adria and is composed of basal Triassic evaporites (Burano Fm), Jurassic–Eocene carbonate-siliceous-marls, Oligocene-Early Miocene marls, clay and arenaceous succession. It oucrops at Circeo Promontory, Zannone Island and Lepini and is found at depth ranging between ~400 and ~2100 m by onshore boreholes (Cretaceous-Miocene succession) near Anzio and south of

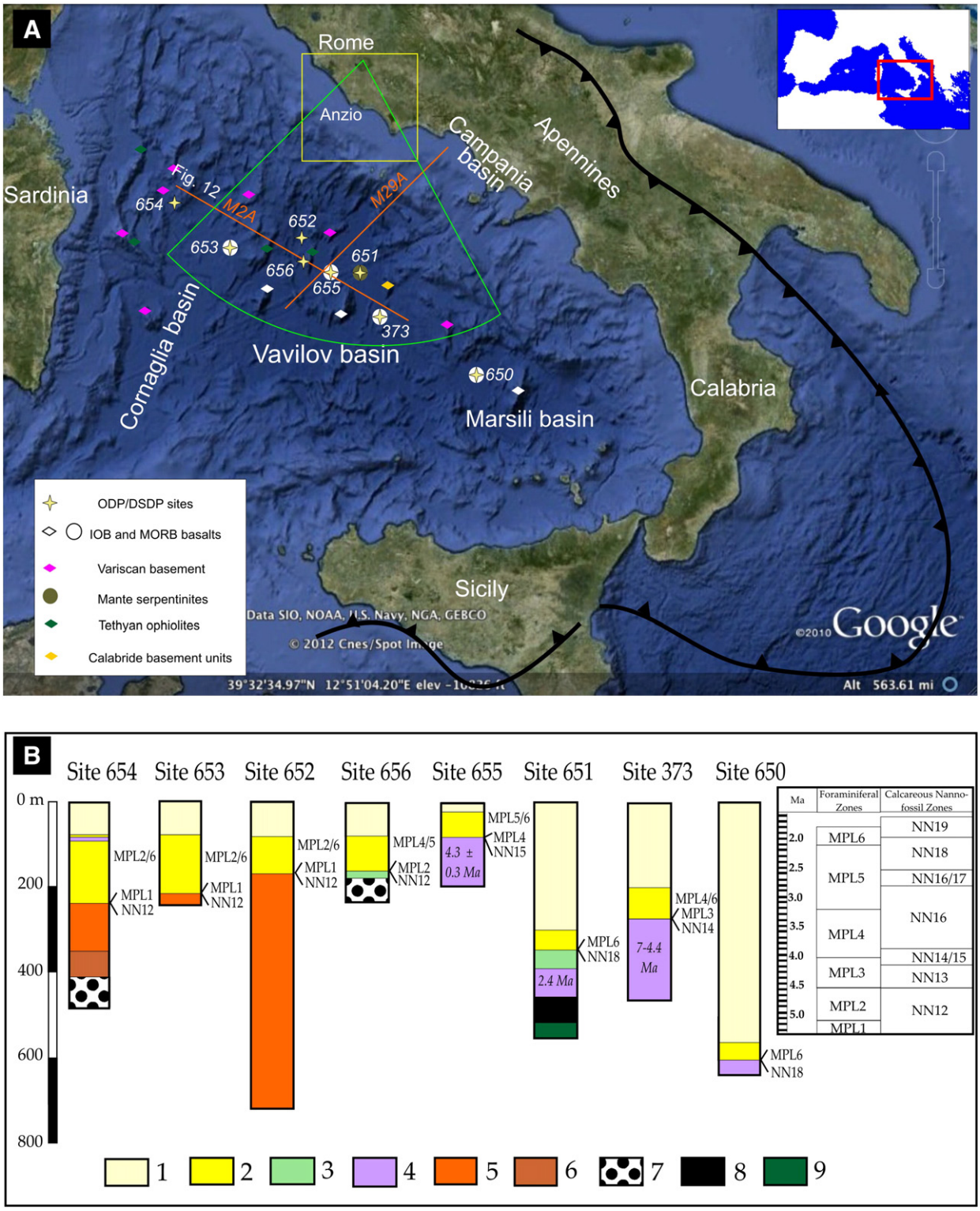

Fig. 1. (A) Index map of Italy and Vavilov basin (green triangle) and location of the M2A CROP profile and DSDP and ODP well sites. The yellow rectangle indicates the location of the area shown in Fig. 2. Bedrock geology is also included and depicted by colored diamonds and circles (Sartori et al., 2004; Sartori, 2005). (B) Stratigraphic logs of the DSDP and ODP sites, modified from Kastens et al. (1987), using the updated Planktonic foraminifer and calcareous nanofossils integrated biostratigraphic scheme for the Mediterranean Pliocene of Violanti (2012). 1) Pleistocene deposits; 2) Pliocene deposits; 3) dolostones; 4) basalts; 5) Messinian deposits; 6) Tortonian deposits; 7) conglomerates; 8) breccias; 9) serpentinized peridotites.

Fig. 2. Index map of seismic grid, ship tracks reported in the text and stratigraphic successions of deep wells from the Latium margin. AR = Ardea basin, TC = Torre Caldara, L2 = Latina2 well, L1 = Latina1 well, FA = Fiume Astura well, MA = Michela well, TR = Tre Cancelli well, AC = Acciarella well. FO = Fogliano well. Stratigraphic logs modified from Lombardi (1968), Malatesta and Zarlenga (1985), Bellotti et al. (1997), ViDEPI (2009). We used the updated Planktonic foraminifer and calcareous nanofossils integrated biostratigraphic scheme (lower inset) for the Mediterranean Pliocene of Violanti (2012).

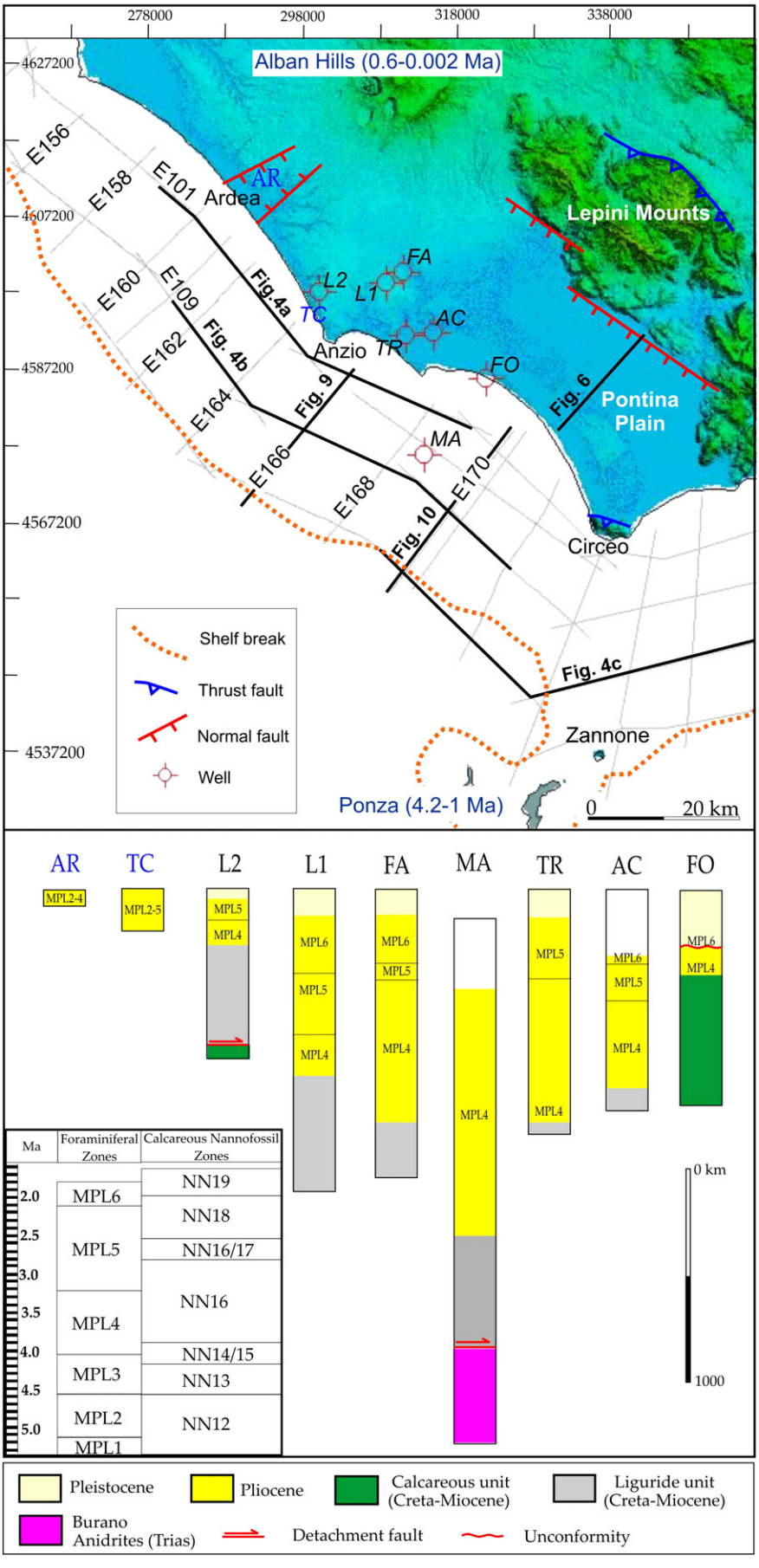
278000
298000
318000
338000
4627200
4607200
4587200
4567200
4537200
Alban Hills (0.6-0.002 Ma)
Ardea
AR
Lepini Mounts
E156
E158
E101
E160
E109
E162
E164
E166
E168
E170
Fig.4a
Fig. 4b
Fig. 9
Fig. 10
Fig. 6
Fig. 4c
FA
L2
L1
TC
AC
Anzio
TR
FO
MA
Pontina Plain
Circeo
Zannone
Ponza (4.2-1 Ma)
0
20 km
Shelf break
Thrust fault
Normal fault
Well
AR
TC
L2
L1
FA
MA
TR
AC
FO
MPL2-4
MPL2-5
MPL5
MPL4
MPL6
MPL5
MPL4
MPL6
MPL5
MPL4
MPL4
MPL5
MPL4
MPL6
MPL5
MPL4
MPL6
MPL4
Ma
Foraminiferal Zones
Calcareous Nannofossil Zones
2.0
2.5
3.0
3.5
4.0
4.5
5.0
MPL6
MPL5
MPL4
MPL3
MPL2
MPL1
NN19
NN18
NN16/17
NN16
NN14/15
NN13
NN12
0 km
1000
Pleistocene
Pliocene
Calcareous unit (Creta-Miocene)
Liguride unit (Creta-Miocene)
Burano Anidrites (Trias)
Detachment fault
Unconformity

Anzio (Triassic evaporites, Michela well). The Paleozoic metamorphic basement of the Latium thrust belt, outcropping at Zannone Island, is covered by the Carbonate unit along a low-angle fault (De Rita et al., 1986), which has been recently interpreted as an extensional detachment fault (Milia et al., 2013).

The Latium Apennine fold-and-thrust belt formed during upper Miocene (e.g., Lepini thrust; Fig. 2) and was overprinted in Lower Pliocene by extensional basins, such as Tiberino, Ardea, and Gaeta Bay basins (Cavinato and De Celles, 1999; Iannace et al., 2013; Milia et al., 2013). The Latium margin includes (Fig. 2) an approximately 100 km-long and 50 km-wide basin extending offshore (Tyrrhenian Sea shelf) and onshore (from Ardea to Pontina Plain). Previous studies of this margin have been based on wells, outcrops and seismic profiles (Malatesta and Zarlenga, 1985, 1986; De Rita et al., 1986; Mariani and Prato, 1988; Faccenna et al., 1994; Bellotti et al., 1997). The basin fill is up to 1500 m thick and formed by thick clastic deposits of Pliocene age, covered by a few hundred meters of Quaternary clastics and tuffs (Lombardi, 1968; Malatesta and Zarlenga, 1985, 1986; Marani et al., 1986; Mariani and Prato, 1988; Bellotti et al., 1997). These deposits, outcropping along the coast near Anzio, have been subdivided into four stratigraphic units (Bellotti et al., 1997). The basal unit corresponds to pelitic and sandy pelitic sediments deposited on a prograding continental shelf during Lower Pliocene. The palegeographic evolution of the Latium margin during Pliocene-Pleistocene times is likely controlled by NE–SW, N–S and NW–SE faults (Malatesta and Zarlenga, 1985, 1986; Mariani and Prato, 1988; Faccenna et al., 1994), but the mechanical relationship between these faults systems is still debated. The volcanic activity of the Latium margin started in Pliocene times at the western Pontine Islands (Palmarola, Ponza and Zannone, 4.2 Ma to 1.0 Ma) (De Rita et al., 1986; Cadoux et al., 2005). This acid volcanism was followed in the Middle Pleistocene by the Alban Hills ultrapotassic volcanic complex (0.63 to 0.02 Ma) (Scrocca et al., 2003a,b). The Alban Hills are part of the Roman Comagmatic Province (Washington, 1906), a NW-striking chain of potassic to ultra-potassic volcanic districts that developed along the Tyrrhenian coast of Italy since Middle Pleistocene time (Serri, 1990 and references therein).

3. Data and methods

We investigated the Vavilov rift zone using 770 km of multichannel seismic profiles (ViDEPI, 2009), well logs acquired in the apex zone (Fig. 2), 500 km of CROP seismic profiles (Scrocca et al., 2003b), ODP, and DSDP wells collected in the distal zone (bathyal Tyrrhenian Basin, Fig. 1). The seismic interpretation has been calibrated using deep well logs and outcrop data. These seismic data were subsequently processed in order to obtain a consistent dataset: seismic line basemaps and well position were geo-referenced in a common coordinate system (European Datum 50) and assembled in a dedicated GIS environment (Kingdom, IHS Inc.). Raster images of the overall seismic profiles were converted to segy format using image2segy, a free tool developed by Farran (Instituto de Ciències del Mar, Barcelona University) for MATLAB software.

We interpreted the seismic data-set using the seismic stratigraphy method (e.g., Mitchum et al., 1977). The seismic units were calibrated using the lithostratigraphic and offshore/onshore chronostratigraphic data. The seismic depth conversion in the Vavilov's apex region was achieved applying the "layer-cake time-depth conversion" model, in which the velocity in one layer can potentially be represented by a constant, through the "Dynamic Depth Conversion" tool of the 2d/3dPAK-EarthPAK module of the Kingdom software. The values of P-waves velocities (V_p) used in the conversion were obtained from the sonic logs of two wells: the Michela well (located offshore) and the Fiume Astura well (located onshore). The raster image of the sonic logs were imported, calibrated and then digitalized to obtain, through the use of specific algorithms, the velocity log (m/s). We performed a review of the stratigraphic units of the Vavilov basin infill present on the stratigraphic logs (Figs. 1, 2) of the ODP/DSDP projects (Hsu et al., 1978; Kastens et al., 1987; Channell et al., 1990) and Latium margin (Lombardi, 1968; Malatesta and Zarlenga, 1985; Bellotti et al., 1997; ViDEPI, 2009), using an updated Planktonic foraminifer and calcareous nannofossils integrated biostratigraphic scheme for the Mediterranean Pliocene (Violanti, 2012). We interpreted faults on seismic reflection profiles, mapped them in a GIS environment, and displayed them as lines on structure contour maps and isochron maps. Although in the apex zone many boundary faults displacing the substrate are buried by thick Pliocene deposits, the high density of seismic lines made it possible to recognize and link major faults based on their geometry, dip direction, and amount of throw. In contrast, in the distal rift zone, characterized by few seismic profiles and underfilled basins, the mapping of the main faults down-throwing the substrate was supported by swath bathymetry data (Marani et al., 2004).

4. Results

4.1. Basin physiography

The main physiographic feature of the Vavilov basin is the triangular geometry of its 3500 m-deep bathyal plain convergent toward the Latium margin (Fig. 1). The margins of the bathyal plain correspond to structural highs made up of metamorphic and sedimentary rocks bounded by NE-SW and NW-SE faults (e.g. Selli Line., Sartori Escarpment). NNE-trending large volcanic seamounts (Magnaghi, Vavilov) occupy the otherwise flat-lying abyssal plain. The Latium margin is characterized by an approximately 20 km-wide continental shelf that is connected to the bathyal plain by a region characterized by an irregular physiography and intra-slope basins (Fig. 1). The onshore Latium margin is formed by a wide plain bounded by the reliefs of the Apennines (Fig. 2). Its structural pattern features Pliocene-Quaternary normal faults trending NE-SW (Ardea basin) and NW-SE (Pontina Plain) that converge into the apex located at the Alban Hills volcano (Fig. 2).

4.2. Apex stratigraphy and basin geometry

The stratigraphy of the apex zone, documented by several deep wells and outcrops, is characterized by a Pliocene-Pleistocene succession that lies unconformably on a variable substrate, corresponding to the Apennine nappes made up of Mesozoic-Miocene carbonate rocks of shelf and margin environment, overthrusted by Mesozoic-Miocene clastic rocks of deep basin environment (Liguride unit) (Fig. 2). On the basis of the planctonic foraminifera, Pliocene deposits have been attributed to the MPL2-MPL6 biostratigraphic zones (Fig. 2). The oldest Pliocene stratigraphic units (MPL2-MPL3) outcrop in the western part of the study area (Ardea basin and Torre Caldara sections; Fig. 2). A thick and younger succession, mainly composed of MPL4 deposits, was encountered in the central part of the study area (Latina 1, Fiume Astura, Martina, Tre Cancelli and Acciarella wells). Notably, in the eastern part of the study area an unconformity separating MPL4 deposits from MPL6 deposits has been recognized (Fogliano well).

The interpretation of the seismic lines, calibrated by wells and outcrops in the apex region, allowed the recognition of a Pliocene-Quaternary succession overlying the acoustic substrate and reconstruction of the architecture of the sedimentary basins and faults. The first step of the seismic interpretation was the identification of seismic stratigraphic units. Individual units were delineated on the basis of stratal termination, lower and upper boundary and internal layering features revealed by seismic reflectivity. The acoustic substrate (Unit L) is characterized by a chaotic seismic facies and bounded at the top by strong reflectors in the western and central parts of the basin; its upper boundary is irregular and disrupted by faults (Figs. 3a, 4). Unit L corresponds to the Cretaceous-Miocene clastic deposits of the Liguride nappe overthrusting the Mesozoic carbonate nappe, as documented by wells stratigraphy (Fig. 2) and onshore geology. In the central basin, Unit L

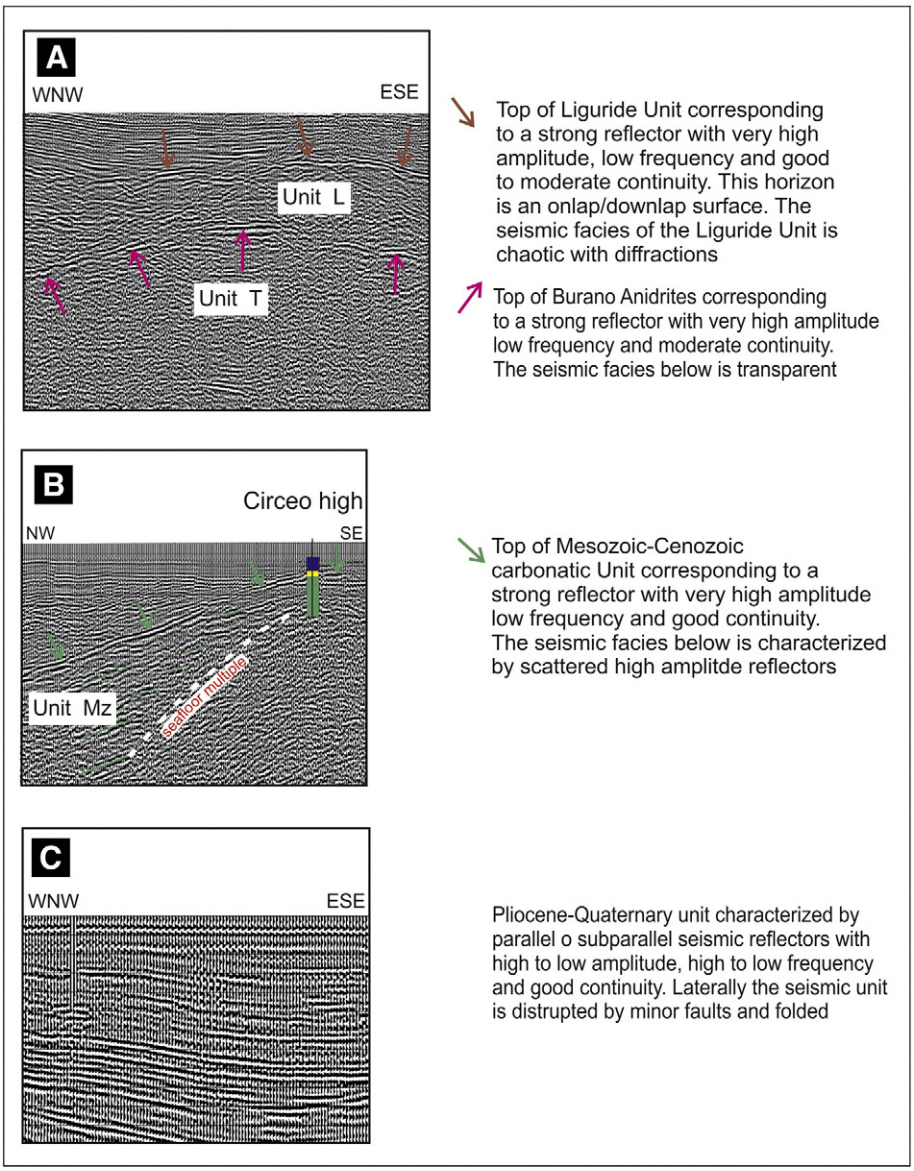

Fig. 3. Close-ups of seismic profiles sectors showing seismic facies types, diagnostic key horizons of the acoustic substrate, and Pliocene-Pleistocene basin fill. For seismic lines location see Fig. 4.

overlays Unit T, characterized by transparent seismic facies. The latter unit presents strong reflectors at the top displaying a convex-upwards geometry (Fig. 3a). The stratigraphy of the Michela well (Fig. 2) reveals that the underlying unit corresponds to Triassic evaporites (Burano Fm) that are the lowermost part of the Apennine carbonate succession, tectonically overlain by the Liguride unit (Fig. 3a). In the eastern part of the Latium Margin, the acoustic substrate (Unit MZ; Fig. 3b) is characterized by isolated strong reflectors with approximately parallel geometry. Its top features a continuous strong reflector with high amplitude and low frequency. This substrate corresponds to Mesozoic-Cenozoic rocks cropping out onshore (e.g. Lepini Mts, Circeo Promontory) and drilled in wells Latina 2 and Fogliano (Fig. 2). In the offshore north of Zannone Island, the acoustic substrate presents a chaotic seismic facies and corresponds to the Paleozoic metamorphic basement rocks (Fig. 4c) outcropping on the island and covered by tectonic slices of Mesozoic-Cenozoic rocks (De Rita et al., 1986).

The acoustic substrate is covered in onlap or downlap by a seismic unit characterized by parallel or subparallel reflectors with variable amplitude and frequency and having good continuity (Fig. 3c). This younger seismic unit corresponds to the Pliocene-Quaternary succession drilled offshore and onshore. The occurrence of angular and erosional unconformities permitted us to recognize several subunits (Fig. 4). Indeed, the well calibration based on foraminifera biozones and stratigraphy of the outcropping geologic section allowed us to divide the Pliocene-Quaternary succession into subunits MPL2–3, MPL4, MPL5, MPL6, and Quaternary (Fig. 4).

In the northwestern area an asymmetrical rift basin filled by the Pliocene-Quaternary succession is present (Fig. 4a–b). The rift basin features NW-dipping and SE-dipping normal faults. This western basin, corresponding to the prolongation of the onshore Ardea basin, displays a thick (up to1 second TWTT) lower Pliocene (MPL2-MPL4) infill, featuring a SE-wards thickening of the wedge that records syn-tectonic fault activity. The western basin develops as a graben bounded by synthetic and antithetic faults near the coast. Seawards its depocenter is shifted and its architecture changes to a half-graben delimited by NW-dipping faults and filled by a clastic wedge (Fig. 4a–b).

In contrast, in the central area a larger and deep sedimentary basin occurs (Fig. 4a–b). The infill of the central basin displays relics of older MPL2-MPL3 sediments, which overlie minor fault blocks and are topped by an erosional truncation. Thick sub-horizontal MPL4 deposits fill the

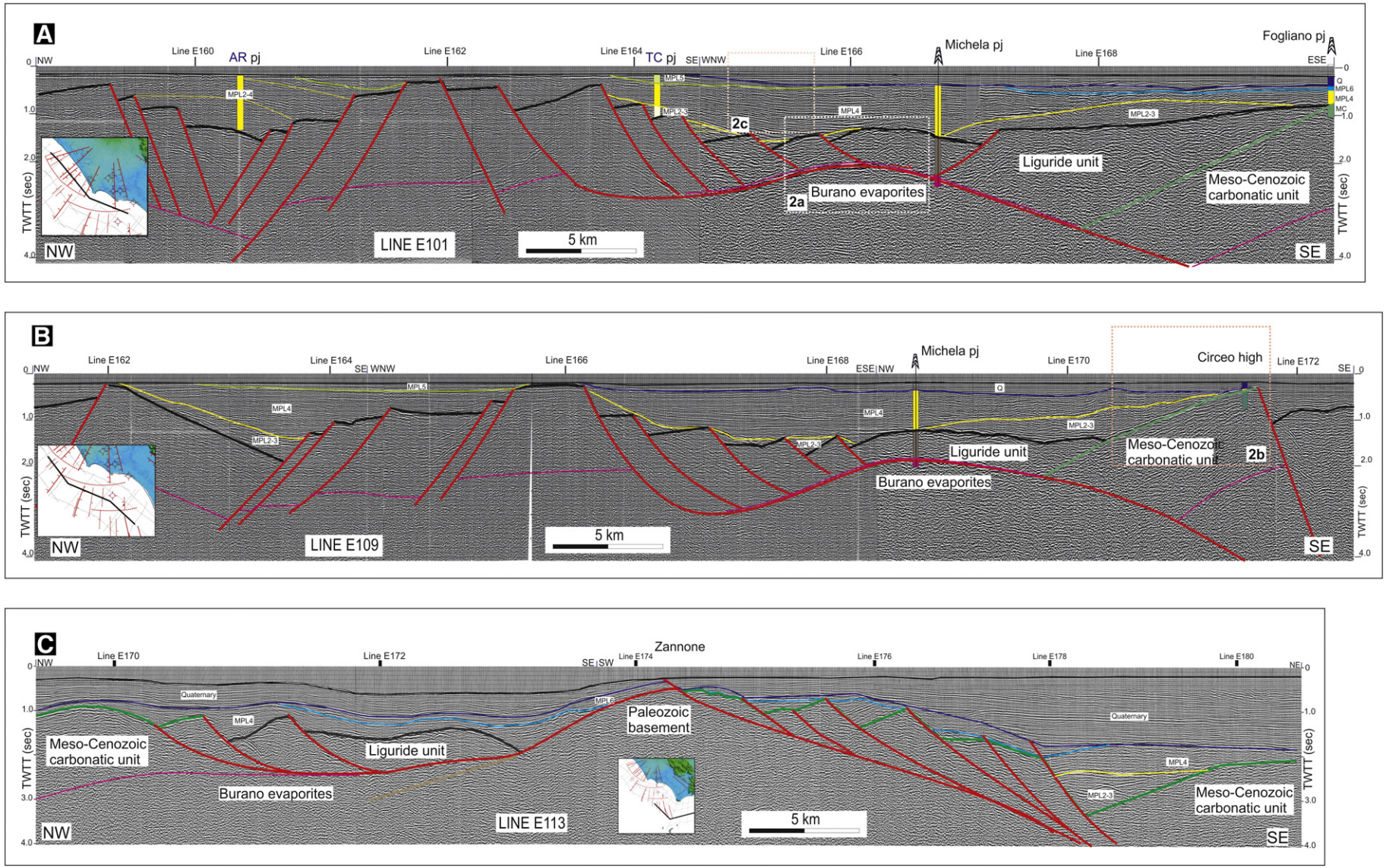

Fig. 4. (A) Interpreted seismic line 101 and its calibration with drilled boreholes located near the profile. (B) Interpreted seismic line 109 calibrated with the Michela well. (C) Interpreted seismic line 111 (modified after Milia et al., 2013). Dotted orange and white boxes delimit the close-ups displayed in Fig. 3.

basin onlapping older deposits and the substrate. The top of MPL4 deposits corresponds to an erosional unconformity. Southwards the central basin displays (Fig. 4c) the MPL4 succession that onlaps the Paleozoic metamorphic basement (outcropping at Zannone Island) and both units are covered by MPL6 deposits. The central basin depocenter is shifted in correspondence of a transform fault (Fig. 4c).

The wells drilled in the axial part of the basin reveal the stratigraphic features of the thick MPL4 succession in the central basin from proximal to distal environments going seawards (Figs. 2, 5). All well logs show a fining-upward trend and a general Transgressive-Regressive cycle of the overall succession, suggesting a subsidence of the basin compensated by sediment supply (Fig. 5). In particular, the Michela well records a 1090 m-thick Transgressive-Regressive cycle deposited over 0.86 Ma and thus a basin subsidence rate of 1.22 mm/y. This value of subsidence rate of the apex region of the Vavilov basin is high compared to the typical synrift subsidence rates (<0.2 mm/y) of stretched basin (Allen and Allen, 2005). In particular, in the proximal area, a relatively thick succession of Transgressive sands overlies basal conglomerates and passes gradually upward to a silts/clays succession. Seaward this succession passes to a thick silts/clays succession with interlayered sand levels that repose on a stratum of sands. The distal deposits correspond to silts and clays interlayered with sands. The trend of the facies and the gamma ray/resistivity logs permit to identify the maximum flooding surface that represents the maximum deepening that the basin experienced. This surface is covered by a coarsening-upward succession, recording a general Regressive trend of the facies. The age of the MPL4 foraminiferal biozone ranges between 4.04 and 3.18 Ma (Violanti, 2012). During this time span a third order depositional sequence formed (Za2 sequence of Snedden and Liu, 2010).

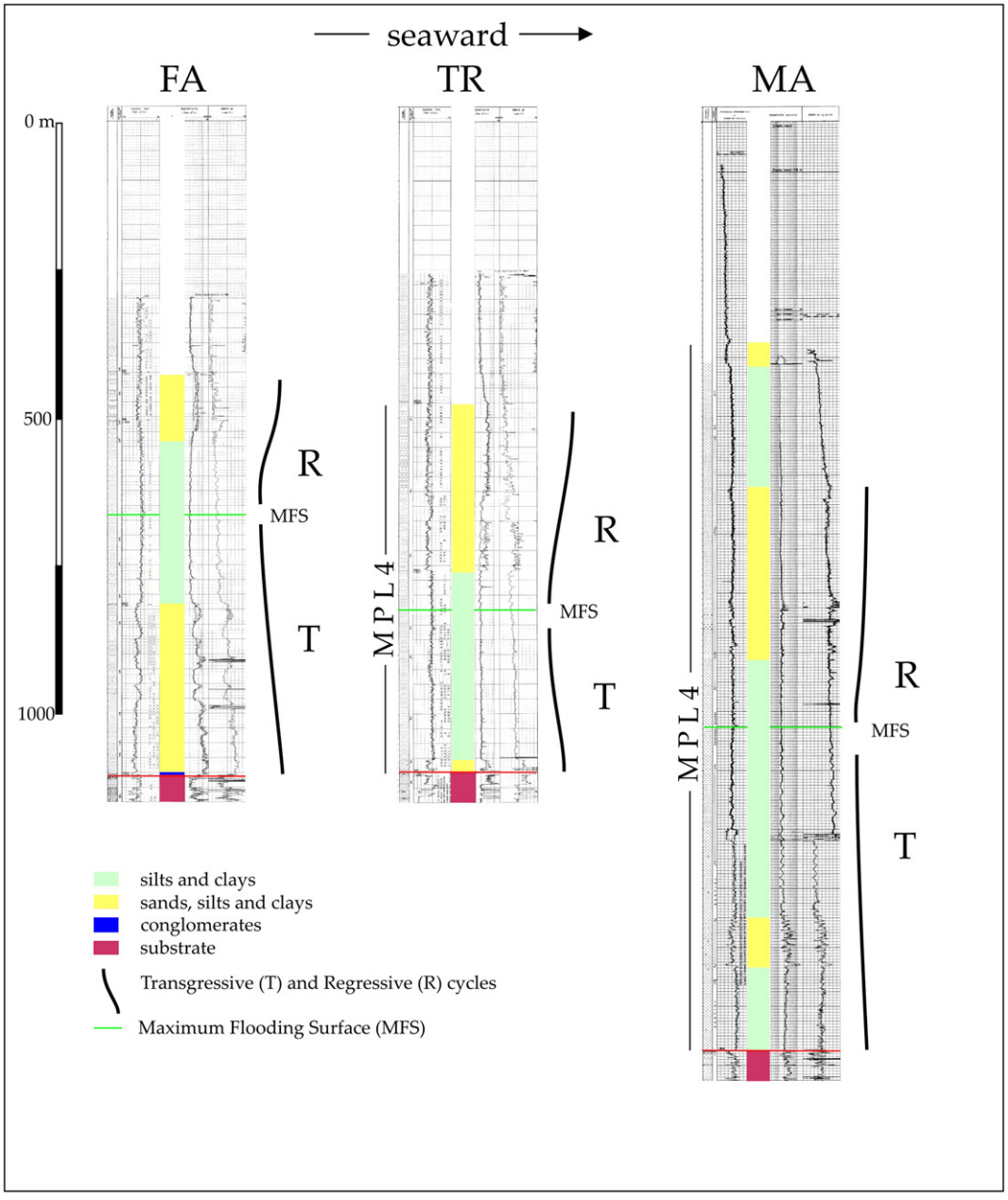

Fig. 5. Geophysical and lithological logs of three wells collected along the axis of the central basin from proximal to distal areas (see Fig. 2 for the location of the well). The log pattern shows characteristic spontaneous potential (SP), lithological log (L) and resistivity (R) signatures for fining upwards (Trangressive cycle) and coarsening upwards (Regressive cycle) units of the MPL4 deposits in the Vavilov apex zone. The Maximum Flooding Surface is recognized based on observed discontinuities or changes in trend of the signature of wireline log records in combination with facies analysis. FA = Fiume Asturia, TR = Tre Cancelli, MA = Michela.

The tectonic omission of the Jurassic-Cretaceous carbonate nappe in the Michela well (that drilled the tectonic contact between Liguride unit and Triassic evaporites) and the occurrence of Mesozoic carbonate tectonic slices above the Paleozoic basement at Zannone Island can be interpreted as the occurrence of an extensional detachment surface in the apex region. Indeed, in regions of high extension, crustal blocks of the upper plate are separated (e.g. Hamilton, 1987). We hypothesize the occurrence of a detachment fault between an upper plate, made up of Ligure unit overlying the Jurassic-Cretaceous carbonate nappe, and a lower plate formed by the Triassic evaporites overlying the Paleozoic crystalline basement. With increasing extension the once continuous carbonate nappe was fragmented into tectonic lenses that slid apart along this detachment. In the last stage, the flat geometry of the detachment was bowed upward and the exhumation of the Paleozoic basement occurred. According to the detachment model, we maintain that the high-angle normal faults bounding the central basin merge into a main listric normal fault dipping SE into the Triassic evaporites (Fig. 4). Due to the high impedance contrast between Triassic evaporitic rocks and clastic deposits of the Liguride unit, a strong sub-horizontal reflector (Fig. 3a) is associated with this low-angle fault that displays a bowed upward geometry, (Fig. 4a–b).

The architecture of the central basin (sub-horizontal strata of the basin fill, >20 km-wide) in the apex area supports its interpretation as a supradetachment basin that formed above a low-angle normal fault system and shows a depocenter located approximately 10 km away from the main bounding fault (Fig. 4).

In the eastern margin (Pontina Plain), there is another half-graben basin filled by two Pliocene sedimentary wedges (MPL4 and MPL6, separated by a tectonically-enhanced unconformity) and a Quaternary tabular unit (Fig. 6). This basin is controlled by NW-oriented normal faults and shows a main fault located at the boundary between coastal plain and Lepini Mountains (Fig. 2).

In order to obtain an isopach map of Pliocene-Quaternary deposits in the Vavilov's apex region, we made a depth conversion of the seismic data. We found the arithmetic average of the P-waves velocities values for the main lithostratigraphic units drilled by the Michela and Fiume Astura wells (Fig. 7). Based on the mean values of P-waves velocities (V_p) obtained from well Sonic Logs, a four-layers velocity model has been adopted for the seismic depth conversion: V_p values of 1500 m/s, 2700 m/s, 3487 m/s and 6138 m/s were assigned to sea water, Pliocene-Quaternary deposits, Liguride Unit and Burano Anidrites, respectively. The structural isopach map (Fig. 8) displays a triangular rift area with three main depocentres: a western basin (approximately 10 km-wide and up to 2000 m-thick), a central basin (approximately 20 km-wide and up to-2400 m-thick), and an eastern basin (Pontina Plain, up to 1000 m-thick). The fault pattern is characterized by normal faults, transfer faults and inversion structures (sensu Cooper and Williams, 1989). The normal faults trend from ENE-WSW to N-S to NW-SE and converge toward a rotation pole located in correspondence of Alban Hills volcano.

4.3. Fault timing in the apex zone

On the basis of the geometry and age of the basin infill, we dated several events of fault activity: (i) the oldest normal faults were active between 5.1 and 4.5 Ma (MPL2-MPL3 succession); (ii) younger normal faults affected the central basin between 4.0 and 3.2 Ma (MPL4 succession); (iii) the normal faults that bound the eastern basin were active until 1.8 Ma (MPL6 succession). The displacement along these normal faults is transferred, or relayed, from one to the next along accommodation zones corresponding to transfer faults. Accommodation zones along major bounding structures are sites of intra-basinal highs, characterized by thinner sedimentary covers (Fig. 9). The transfer faults, orthogonal to the normal faults, offset the basin depocenters (Fig. 8). A positive inversion structure located near a transfer fault deforms the central basin rift. Indeed the thick MPL4 deposits, bounded by N-S normal faults, are shortened to form an antiform, overlying sub-horizontal strata. These observations suggest that some of the pre-existing faults are successively inverted (Fig. 10). The transfer faults formed during the extensional phases and were reactivated after the deposition of the MPL4 deposits. The age of this inversion tectonics can be correlated to the stratigraphic gap (between MPL4 and MPL6) in the Fogliano well succession (Fig. 2) that in turn can be interpreted as a tectonically-enhanced unconformity.

4.4. Distal stratigraphy and basin geometry

The Vavilov rift zone (Fig. 11) shows a converging pattern of normal faults bounding submarine ridges, from west to east: (i) the NE-SW Central Fault (Selli Line), bordering the western part of the bathyal basin; (ii) the NNE-SSW De Marchi seamount, consisting of an extensional allochthon composed of Tethyan ophiolitic rocks, parallel to a couple of normal faults controlling a Pliocene-Pleistocene depocenter (thickness > 1 km); (iii) the N-S Gortani ridge, composed of basaltic rocks, bounding the largest depocenter of Pliocene-Quaternary deposits (thickness > 1 km) in the central bathyal area; (iv) a NW trending ridge, separating the bathyal zone from the eastern Tyrrhenian continental margin.

Several studies of the Tyrrhenian Sea described the stratigraphy and main structural features of this basin. However, the interpretation of the CROP seismic data, calibrated by ODP wells and dredges, provides a new picture of the Tyrrhenian rifting, characterized by a complex basin architecture (Fig. 12). The identification of the sedimentary basin fill and substrate permitted us to attribute an age to the basin formation. Early Pliocene sediments (MPL1) were deposited west of the De Marchi Smt. In the Cornaglia basin the MPL1 unit forms an isopach postrift layer that overlies in stratigraphic continuity thick upper Miocene synrift sedimentary wedges. Between the Central Fault and the De Marchi Smt a younger basin, bounded by normal faults displacing Pliocene deposits, shows in the middle (ODP site 656) the MPL2 unit overlying Messinian deposits. East of the De Marchi Smt instead younger Pliocene deposits (MPL4-MPL6) fill the central bathyal plain.

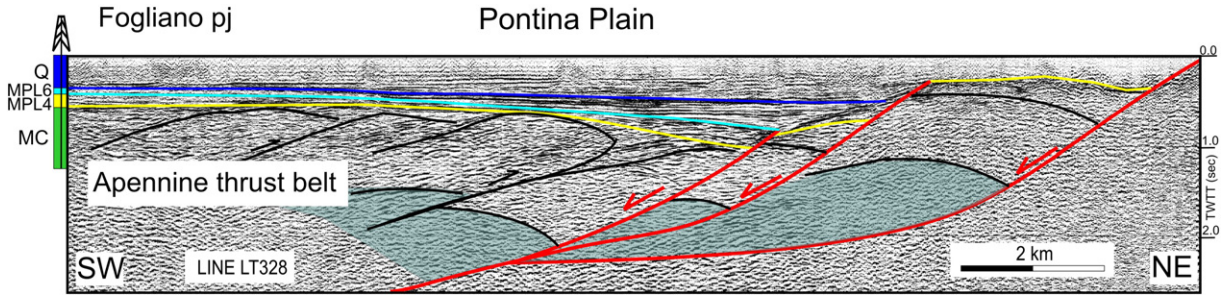

Fig. 6. Interpreted seismic line across the Pontina Plain, calibrated with the stratigraphic log of the Fogliano well, showing a Pliocene-Quaternary basin bounded by SW-dipping listric normal faults (modified from Milia and Torrente, 2015a). This basin is overprinted on the Apennine thrust belt formed by Mesozoic-Cenozoic rocks. For seismic line location see Fig. 2.

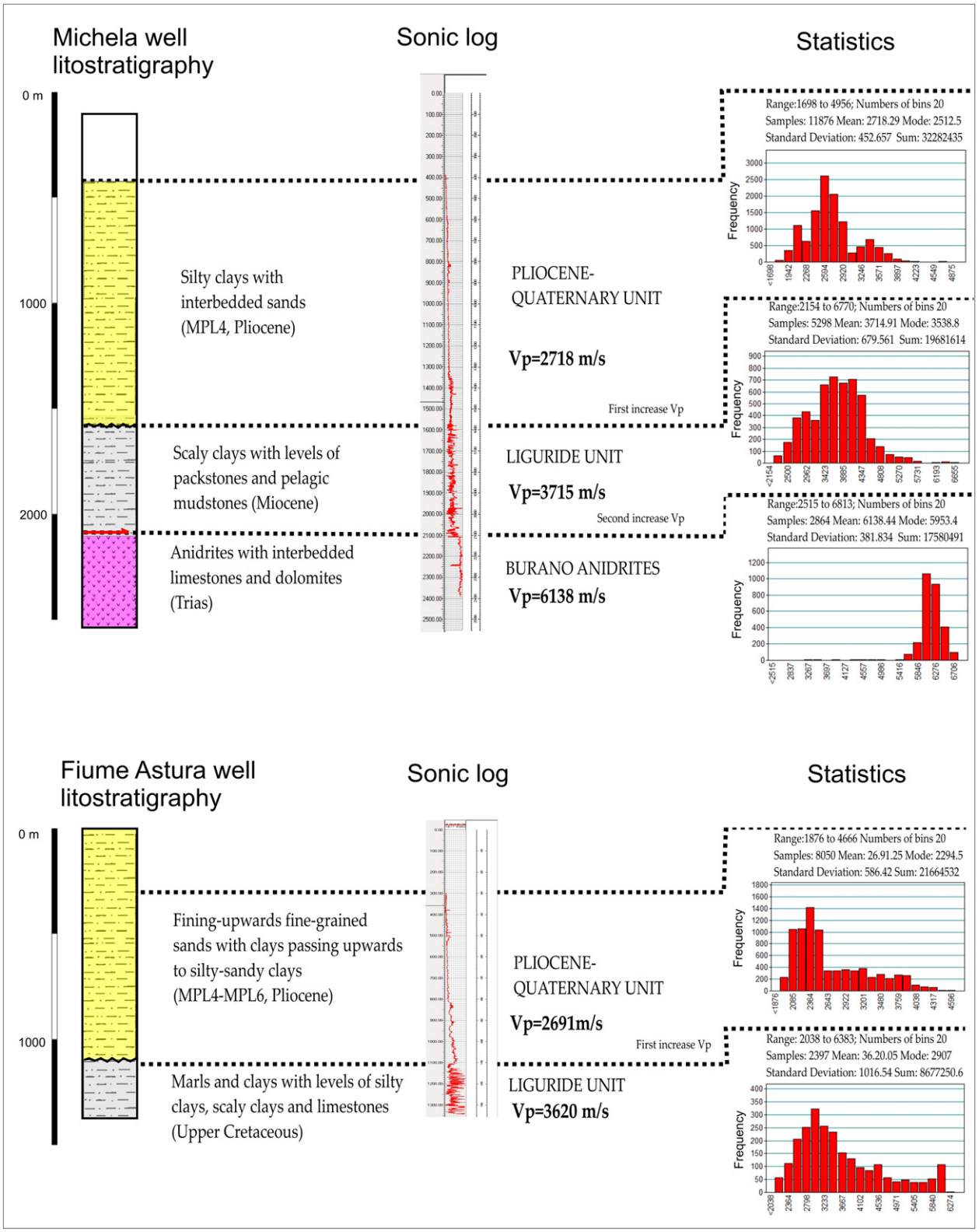

Fig. 7. Lithological and sonic logs of Michela and Fiume Astura wells (see Fig. 2 for well location). The right panel displays a statistical analysis of the velocities of the Pliocene-Quaternary deposits, Liguride Unit and Burano Anidrites.

Even if it is not possible to detect strong reflectors in the deeper part of the CROP seismic profiles, we have evidence of the basal extensional detachment in the bathyal zone from the drilling of the ODP 651 site (Fig. 12). On the basis of this tectonic constraint, we propose an interpretation of the extensional fault system and a crustal geological model of the Vavilov basin characterized by: high-angle normal faults linked to a basal detachment, rift, and supradetachment basins (Fig. 12). More in detail, the overall fault pattern of the Vavilov distal region is characterized by two sets of structures (Fig. 12): older faults, mainly formed west of the De Marchi Seamount and younger faults, active

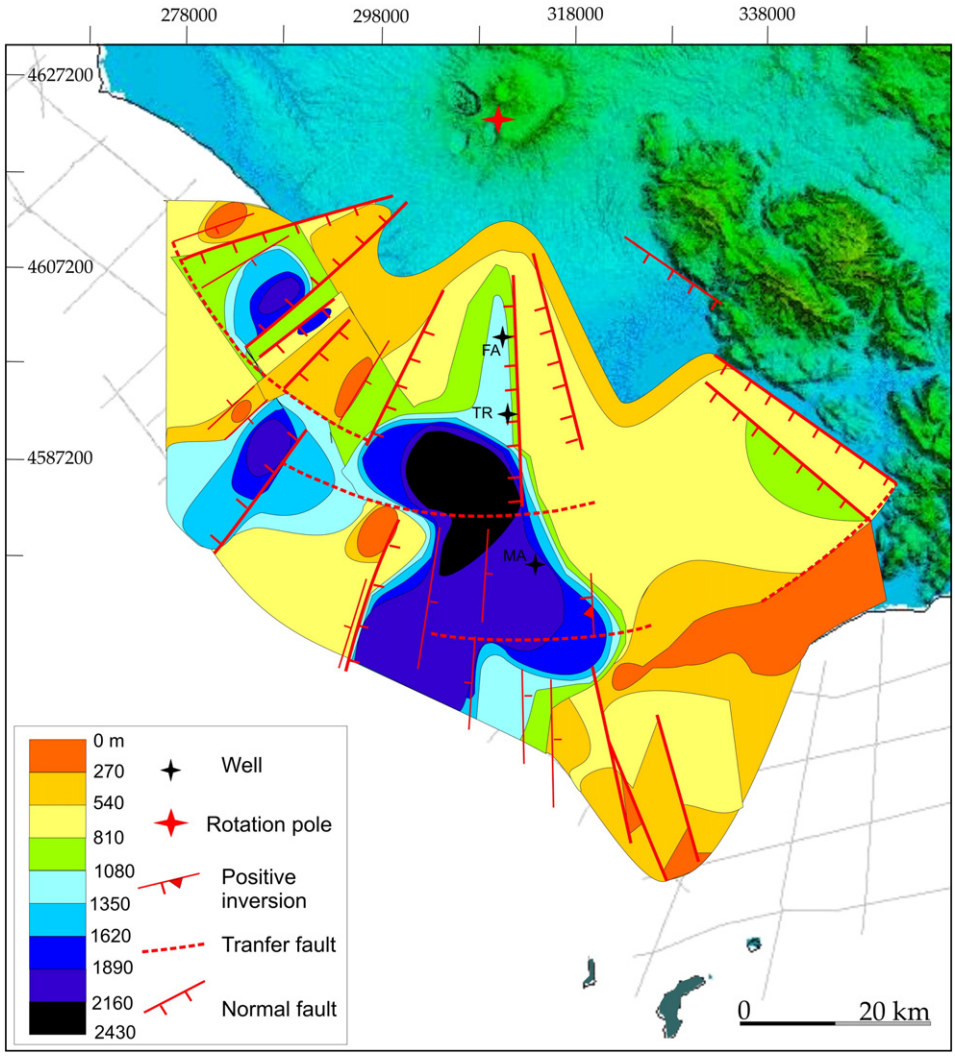

Fig. 8. Structural map of the Latium margin and thickness map of Pliocene-Quaternary deposits. FA = Fiume Astura, MA = Martina, TC = Tre Cancelli. Thickness values are estimated merging well and seismic reflection data. For the depth conversion of Pliocene-Pleistocene seismic units we assumed an average V_p of 2700 m/s.

during detachment faulting, located east of the De Marchi Seamount. The older faults form symmetrical extensional basins characterized by tilted blocks and syn-sedimentary wedges. The younger faults (MPL4-MPL6) are instead associated with a supradetachment basin located east of the De Marchi Seamount. They are linked to a concave-downward main normal fault dipping southeastwards, corresponding to a

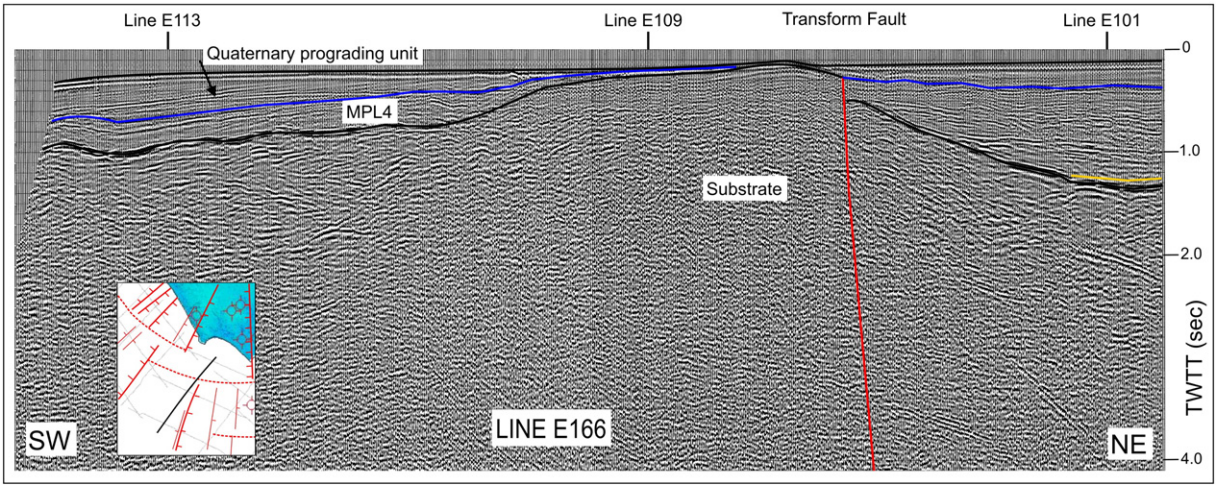

Fig. 9. Interpreted seismic profile 166 showing a transform fault bounding a structural high.

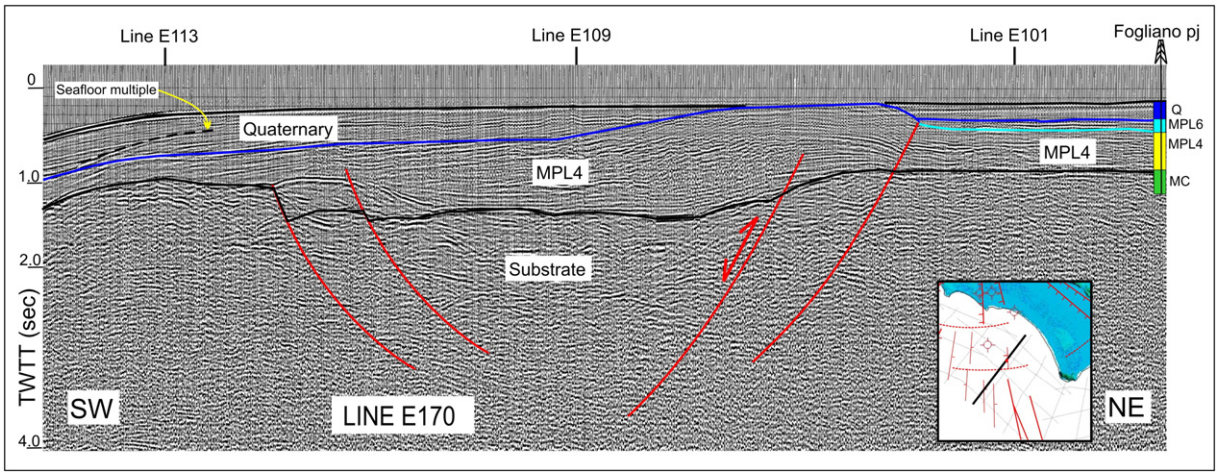

Fig. 10. Interpreted seismic profile 170 displaying a positive inversion structure.

detachment surface (drilled at site 651) that displaced the entire crust and upper mantle, and led to the exhumation of serpentinized peridotites. East of the De Marchi Seamount, a central bathyal plain (drilled at sites 655, 651, and 373) is located. This area is characterized by the absence of major topographic highs, except for the volcanic reliefs of the Gortani ridge and Vavilov volcano (Fig. 1).

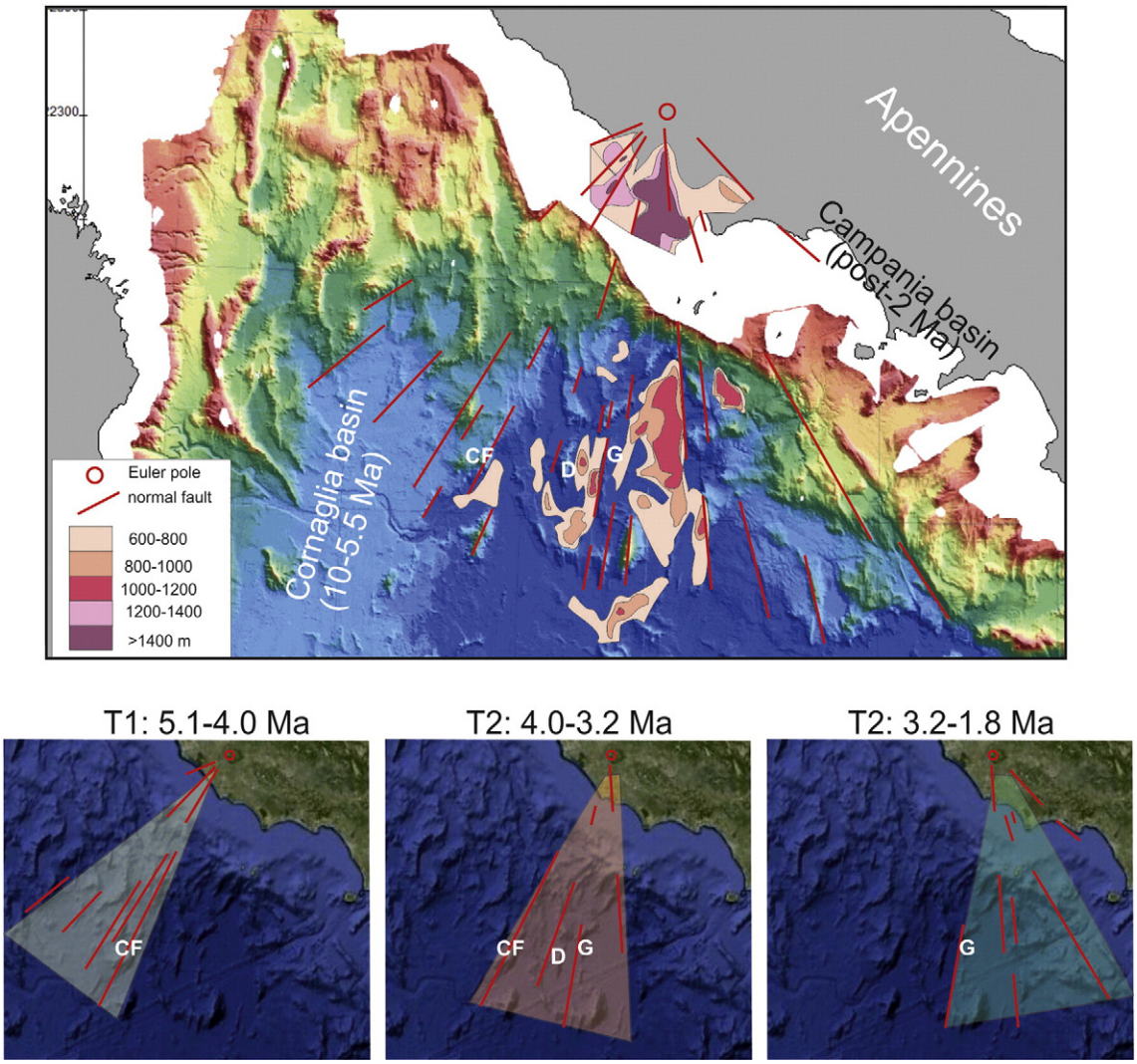

Fig. 11. Pattern of normal faults and thickness map of Pliocene-Pleistocene deposits displaying the triangular geometry of the Vavilov rift zone; CF = Central Fault, D = De Marchi Seamount, G = Gortani Ridge. Thicknesses of the distal region are from Sartori et al. (2004) and seafloor morphology is from Marani et al. (2004). The lower diagrams show the eastwards time migration of extension in the Vavilov basin.

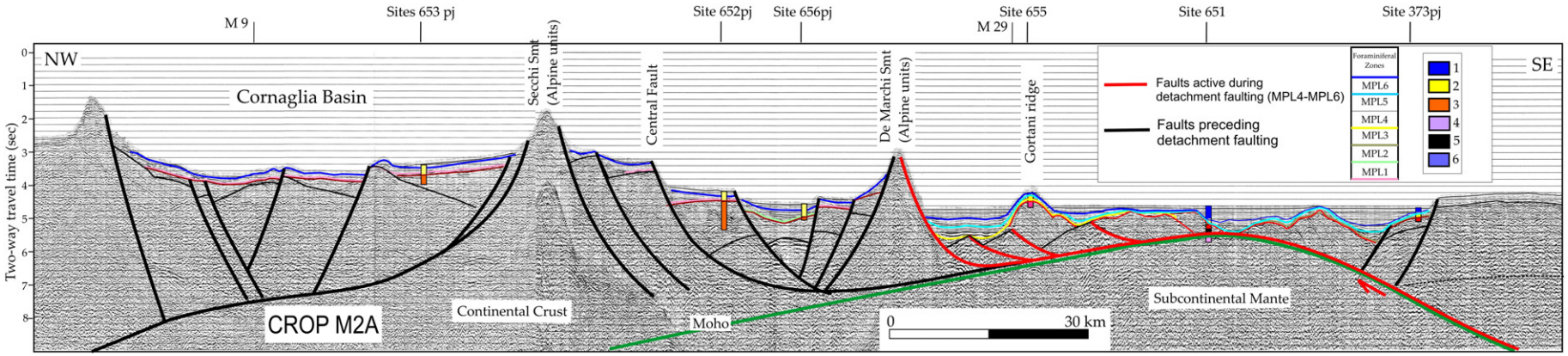

Fig. 12. CROP seismic profile M2A and interpretation. 1) Pleistocene deposits; 2) Pliocene deposits; 3) Messinian deposits 4) basalts; 5) breccias; 6) serpentinized peridotites. For profile location see Fig. 1. See text for explanation.

5. Discussion

Here we use seismic stratigraphic and structural methods to interpret the basin architecture and evolution. Indeed, the age, distribution and pattern of the sedimentary infill is strictly controlled by the development of the normal faults. The variety of structural geometries and their effect on the sedimentation and evolution of the sedimentary fill have been used to interpret the main structural elements at depth. The interpretation of the data discussed in the previous section in a framework provided by the European crustal model EuCRUST-07 (Tesauro et al., 2008), enables us to analyze the link existing between the crustal structure and basin evolution. In this way, we obtain a complete picture of the tectonic evolution of the region, lacking so far.

5.1. Kinematic evolution

We propose a kinematic model for the Pliocene Tyrrhenian rift development based on the premise that age and architecture of the sedimentary basins and faults bounding the basins provide snapshots of a regional continuous extensional process (Figs. 13–14). The wedge-shaped Miocene deposits of the western area of the Tyrrhenian Sea record the opening of the N-S elongated Cornaglia Basin (Sartori et al., 2004). They are covered by Early Pliocene (MPL1) postrift deposits, which are absent in the apex region (Apennines) and distal area east of the De Marchi Smt. The Vavilov rifting, started in the Lower Pliocene (MPL2–3), produced a system of graben/half graben bounded by high angle normal faults that displaced the Latium margin and the distal area west of the De Marchi Seamount. These basins were affected by continuous subsidence and, in the area close to the coast, were filled by thick clastic deposits. With increasing extension, the development of low-angle normal faults resulted in the formation of new sedimentary basins filled by a middle Pliocene (MPL4) sedimentary succession. The activity of detachment zones is documented by the deposition of basin-wide horizontal strata in both apex and distal areas.

A kinematic evolution of the rift zone characterized by rift basins followed by supradetachment basins is compatible with the Present geometry of the thrust belt in the apex region. Indeed, the original thrust belt architecture of the Apennine preceding the extensional processes was made up of Liguride nappe overlying Carbonate nappe (Fig. 13a). Successively, the rifting process affected these stacked tectonic units with high-angle normal faults that root downward into the Triassic evaporites (Fig. 13b). We suggest that with the increase of extension, these high-angle faults linked and merged into a basal low-angle detachment, whose activity produced the Carbonate Nappe lateral segmentation and the direct superposition of the Liguride unit above the Triassic evaporites (Fig. 13c). This stage records the formation of a supradetachment basin, showing sub-horizontal strata developed in correspondence of the detachment fault that roots in the Triassic evaporites. Progressive lithospheric extension resulted in thinning of the upper crust, as the detachment fault affected the Palaeozoic metamorphic basement, which was bowed upward (Fig. 13d). At this time a fast uplift occurred, probably due to isostatic adjustments. A similar kinematic style (rift basins followed by supradetachment basins) has been proposed for the upper Miocene evolution of the Paleo-Tyrrhenian Sea (Milia and Torrente, 2015b).

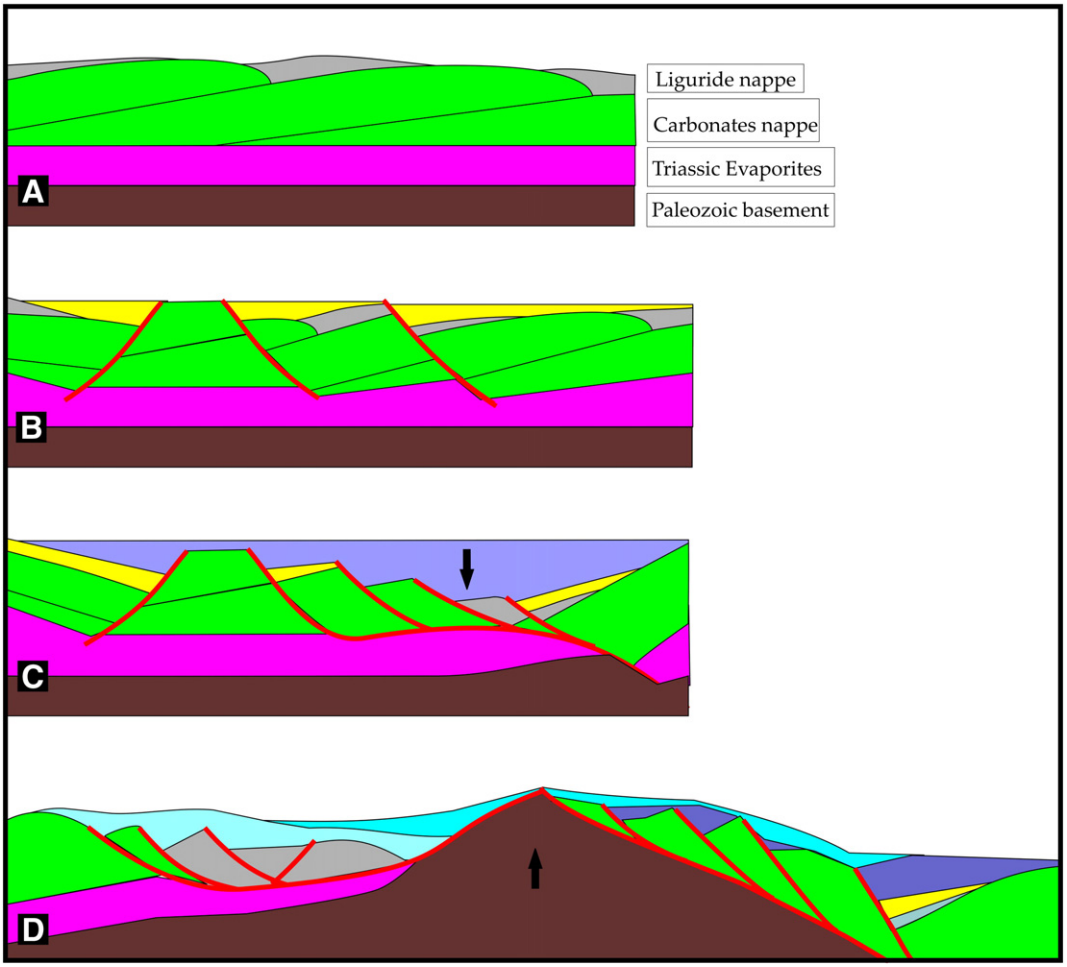

Fig. 13. Cartoon (not scaled) showing three-stage kinematics of the apex rift region. See text for further explanations.

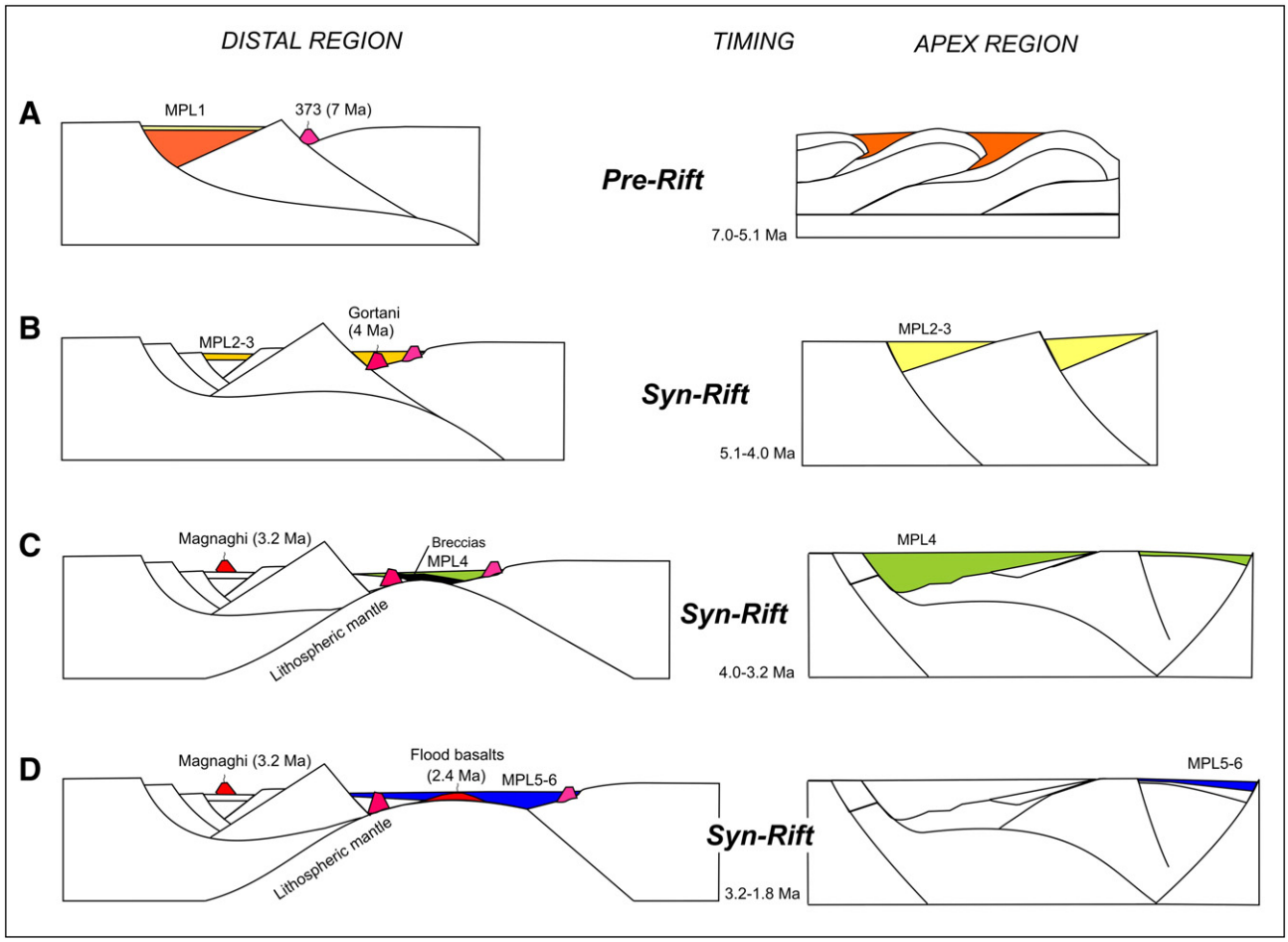

Fig. 14. Interpretative sketch (not scaled) displaying envisaged evolution of the Vavilov rift zone.

The study of the basin fill geometry and fault architecture from apex to distal zones enables us to construct a 3D kinematic model for the Vavilov triangular basin that links extension and volcanism (Fig. 14). The convergent pattern of normal faults (Fig. 11) is coherent with a single Euler pole, located in Latium, during the entire basin history. The kinematics of the Vavilov region records the complete evolution of a rift from stretching to mantle exhumation and the development of rift basins, followed by supradetachment basins (Fig. 14). During the Messinian-early Pliocene (7.0–5.1 Ma; Fig. 14a), MPL1 postrift sediments were deposited at the top of upper Miocene syndepositional wedges only in the distal region on the Sardinia margin. Basaltic volcanism started in the bathyal plain at DSDP site 373.

The age of the sedimentary infill documents that the Vavilov basin started to open in the Lower Pliocene (5.1–4.0 Ma; Fig. 14b) coherently from the apex to distal regions by a pure shear mode, characterized by distributed high-angle normal faulting and asymmetric/symmetric rift basins displaying MPL2-MPL3 syn-kinematic wedges. We maintain that rifting lasted 5.1–4 Ma and thereafter a detachment basin evolved from 4 to 1.8 Ma. The extension switched during the upper Pliocene (Fig. 14c) to a simple shear mode, associated to detachment faults. A supradetachement basin formed in the apex rift zone, which is characterized by strong subsidence and thick sub-horizontal MPL4 deposits featuring a Transgressive-Regressive cycle. In contrast, thin deposits are present in the basin distal zone, due to the increase of the distance from the sediment source area (Apennines). In the distal zone the extension produced a tectonic breccia (site 651), including clasts of deformed early Pliocene deposits and serpentinized peridotites, indicating that the detachment fault cut the upper mantle. During this stage two basaltic volcanoes formed: the Magnaghi seamounts and the Gortani ridge.

The final stage of opening of the Vavilov basin developed by a simple shear mode in the Upper Pliocene (3.2–1.8 Ma) when MPL5-MPL6 deposits were laid down (Fig. 14d). The activity of detachments caused the maximum thinning and exhumation of serpentinized peridotites of the mantle in the distal zone and metamorphic basement rocks in the proximal one. The bowed upwards detachment geometry in the apex area suggests a rapid uplift of crustal rocks that can be explained by isostatic adjustments. Similarly, in the Vavilov distal zone the detachment fault that exhumed mantle rocks displays a downward concave geometry. A downward concave geometry of detachment faults has been predicted in magma-poor extensional margins by numerical experiments and constrained by geological and geophysical observations (Whitmarsh et al., 2001). In particular, the model of Lavier and Manatschal (2006) demonstrates that (1) the flow of the middle part of the crust in the initial stage of rifting and (2) serpentinization of the upper mantle during its last exhumation phase, are the two processes that likely weaken the lithosphere and can explain the rifting evolution, with the establishment of a concave-downward fault. The volcanic activity during the final stage of opening of the Vavilov basin was characterized by small patches of lavas (flood basalts), erupted directly onto the exhumed detachment surfaces. This scenario of MORB basalts, overlying detachment faults and dykes intrusions, is typical of magma-poor rifted margins, as observed in the Indian Ocean (Sauter et al., 2013).

5.2. Crustal structure of the Vavilov basin and geodynamical implications

The heterogeneous crustal structure of the Vavilov basin is shown by the two cross-sections derived from EuCRUST-07 (Fig. 15). This model was constructed assembling a significant number of seismic data

provided by refraction, reflection, and receiver function studies. It provides the depth of the main crustal boundaries and velocities of the upper and lower crust on a uniform grid 15'×15' (Tesauro et al., 2008). We can observe that in the apex region of the basin the crust has a thickness of 20–25 km and two crustal layers with distinct seismic velocities typical of extended continental crust (cross-section 1; Fig. 15). The crust thins and decreases its average velocity toward the bathyal part of the basin quite abruptly (>10 km and ~0.3 km/s over a horizontal distance of <100 km). The thinning occurs approximately in correspondence of the updoming and exhumation of the Paleozoic metamorphic basement (Fig. 4c), which is likely an effect of isostatic adjustment, as a consequence to the decrease of crustal thickness. The crust in the bathyal region of the basin is quite homogeneous (cross-section 2, Fig. 15), being characterized by a uniform thickness of ~7 km and low seismic velocities (V_p ~ 6 km/s) compared to deeper serpentinised peridotite. These results agree with recent seismic refraction interpretation (Prada et al., 2014). The increase of crustal thickness and average velocity toward the Sardinian and Calabrian margin is much smoother (~10 km and 0.3 km/s over a horizontal distance of ~150 km) than toward the apex of the basin. Such a difference in the crustal thickness variations can be ascribed to a change in the crustal strength during the rifting. The higher extension rate in the central part of the basin has caused larger temperature in this area than in the apex during the opening phase. Consequently, the crustal brittle-ductile transition has migrated at shallower depth in the bathyal region, as observed from the faults pattern (Fig. 11). Therefore, the thinning of the brittle part of the crust in this area is responsible for the smoother transition of the crustal thickness.

Assuming an average crustal thickness preceding the formation of the Vavilov basin of ~35 km and mean values of the crustal thickness of ~22 km and ~10 km in the apex and bathyal region the corresponding stretching factor β is ~1.5 and ~3.5, respectively. This difference in the stretching value has significant implications on the crustal type flooring the Vavilov basin. In the northern part of the basin, the limited extension could only modestly thin the continental crust. In contrast, the stronger extension affecting the southern part of the basin could have led to full continental break-up with the consequent formation of oceanic crust, as sustained by some studies (Kastens and Mascle, 1990; Mascle and Rehault, 1990; Sartori, 1990, 2003; Marani and Trua, 2002; Nicolosi et al., 2006) or may have only modified the original continental crust in a transitional type (Panza and Calcagnile, 1979/1980; Florio et al., 2011; Milia et al., 2013; Prada et al., 2014). The low crustal seismic velocities in the bathyal region can be representative of either continental or oceanic rocks, as well as serpentinized peridotite (Christensen and Mooney, 1995). Therefore, these data alone cannot uniquely identify the crustal type characterizing this area, but can be helpful in supporting hypotheses on its crustal nature.

Combining different geophysical data, Prada et al. (2014) interpreted the low crustal velocity as due to the serpentinized upper mantle, locally intruded by basalts. However, they did not detect the boundaries between the extended continental crust and exhumed upper mantle, neither make hypotheses on the time and cause of the upper mantle exhumation. We suggest that the final stage of opening of the Vavilov basin was characterized by the activity of a detachment, maximum thinning and exhumation of serpentinized peridotites of the mantle, simple shear mode (sensu Whitmarsh et al., 2001), covered

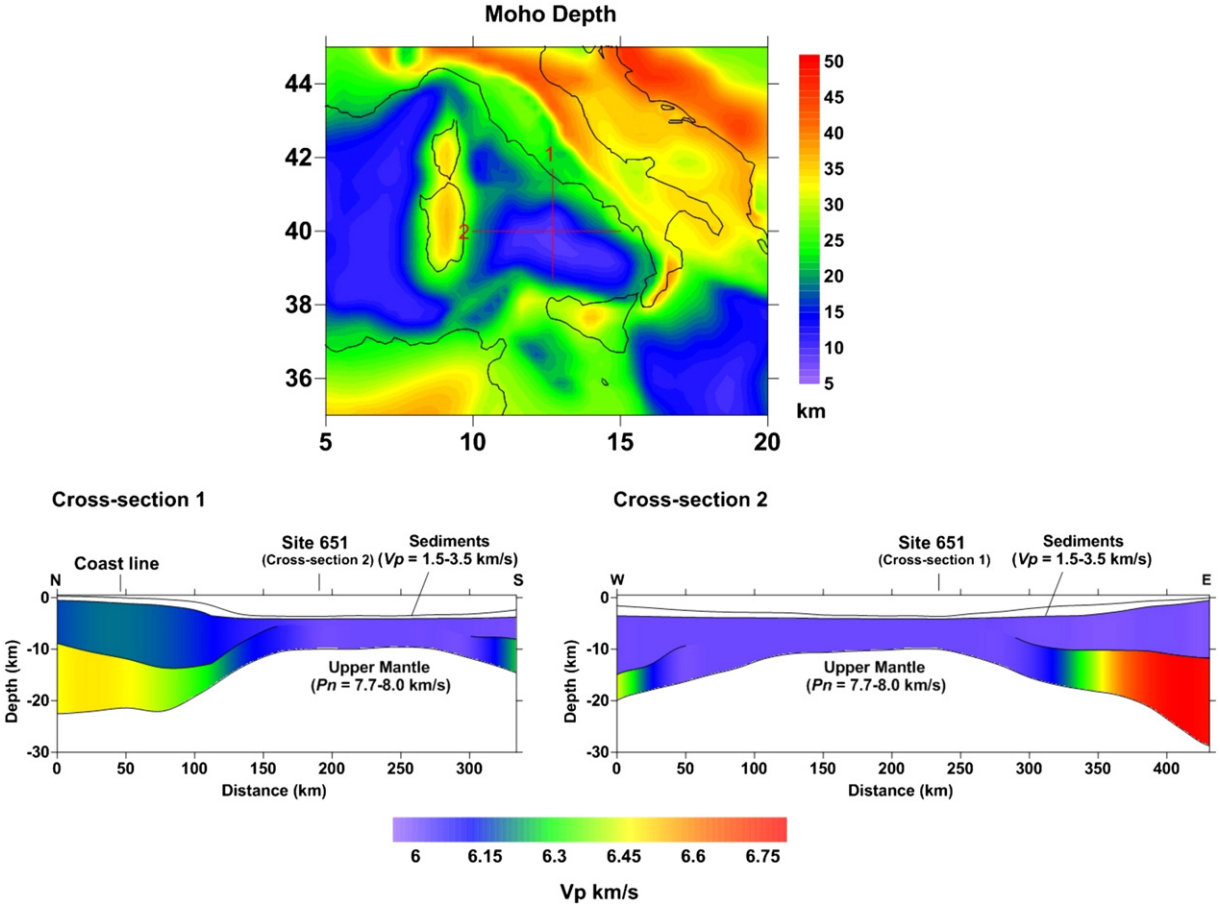

Fig. 15. Moho depth of the Tyrrhenian Sea and surroundings according to the crustal model EuCRUST-07 (Tesauro et al., 2008). Red lines depict location of two cross-sections of EuCRUST-07, displaying the crustal thickness and P-wave velocity variations in the Vavilov basin. Sedimentary thickness and P-wave velocity variations are derived from the interpretation of the seismic reflection profiles. *Pn* values are from Cassinis et al. (2003).

by basalts 2.4 Ma old and MPL6 deposits. On the basis of the interpretation of the CROP seismic lines (Fig. 12), we propose that the mantle rocks have been exhumed along a downward concave fault plane. A similar geometry is common in magma-poor extensional margins, as demonstrated by numerical experiments (Whitmarsh et al., 2001; Lavier and Manatschal, 2006). These models support the formation of exhumed upper mantle during the final stage of continental extension. Mantle serpentinization occurs during margin formation when seawater comes in contact with cold lithospheric mantle rocks (<600 °C). This can occur during extension when the crust is progressively cooled. At this stage, crustal scale faulting becomes possible and can provide the pathways for seawater to reach and react with cold mantle rocks, causing their serpentinization. According to some studies (Hauser et al., 1995; O'Reilly et al., 2006; Reston and Pérez-Gussinyé, 2007), embrittlement of the crust (and thus water ingress and serpentinization) is favored when the upper and middle crust is more extended than the lower crust and upper mantle. Where the upper part of the crust is extended more than its lower part, its heat production will be strongly attenuated, leading to a reduction in lower crustal temperatures and greater likelihood of embrittlement. Such a difference in the stretching value of the crust has been invoked to explain the formation of a moderately serpentinized (<25%) upper mantle, beneath the Porcurpine and the Southern Rockall basins of the North Atlantic margin (Hauser et al., 1995; O'Reilly et al., 2006).

The peridotite sampled at the Site 651 has been subjected to different episodes of hydrous metasomatism/metamorphism. The first one occurred at relatively high temperatures (>700 °C) at the depth of the upper mantle and was likely induced by the fluids released by the subducting Ionian plate. The successive episodes of hydrous metasomatism occurred at crustal levels, at progressively lower pressure and temperatures, during the ascent of the peridotite (Bonatti et al., 1990). Uplift of the peridotite body is also supported by its sequence of high-temperature foliation-low-temperature foliation-brittle deformation (Bonatti et al., 1990). The current prevalence of low-temperature hydrated silicates, such as lizardite and chrysotile, and the scarcity of antigorite suggests that the highest degree of serpentinization was very likely caused by seawater circulating at shallow crustal depth at a temperature not higher than a few hundred degree (Bonatti et al., 1990). Therefore, differently from other extensional basins (e.g., in the Porcurpine and the Southern Rockall basins), where the serpentinized peridotite constitutes a high velocity layer (V_p > 7.2 km/s) underlying the crust at a depth of ~10 km (Hauser et al., 1995; O'Reilly et al., 2006), in the Vavilov basin the upper mantle is exhumed at much shallower depth and almost exposed at the seafloor at the site 651 (Fig. 12). Thus, the extension in the bathyal region of the Vavilov basin caused a more significant crustal thinning and the exhumation of a more serpentinized upper mantle than in the magma-poor continental margins. On the basis of the low seismic velocities observed (V_p ~ 6.0 km/s, Fig. 15), we can estimate that the peridotite reached an average degree of serpentinization around 50%–60% (Christensen, 2004). Exhumation of the upper mantle at very shallow depth and its pervasive serpentinization has been observed in magma poor rifted margins (e.g., Iberian plain) during the last stage of continental extension preceding Oceanization (Chian et al., 1999; Whitmarsh et al., 2001). In contrast, the magmatic activity in the Vavilov basin, leading to flood basalts emplacement over the exhumed upper mantle, followed by the formation of the Vavilov volcano, was not sufficiently voluminous for the formation of real oceanic crust. The crystalline crust flooring the bathyal region of the Vavilov basin is instead a transitional type, composed of serpentinized upper mantle, overlain by volcanic products and thin continental crust west of the De Marchi seamount (Fig. 12). This heterogeneous crust is seismically uniform, characterized by the absence of intra-crustal discontinuities (Fig. 15). Oceanic crust formation could have likely occurred only if extension had persisted in the same area, as in the Iberian plain (Chian et al., 1999; Whitmarsh et al., 2001) or would have been faster. Actually, serpentinites are also typical of abyssal plains surrounding slow spreading ridges (<5 cm/y), which are characterized only by episodic magmatic activity. In contrast, the fast spreading ridges (>9 cm/y) are characterized by a more significant magmatic activity, which leads to the formation of a thick oceanic crust (Deschamps et al., 2013).

The maximum extension of the Vavilov basin occurred in a circa 100 km-wide belt of the bathyal area, bounded by a NE-SW normal fault located west the De Marchi seamount and a N-S normal fault located near the 373 site. The substrate of this belt corresponds to exhumed mantle and not continental crust, thus implying a total amount of extension in the Vavilov rift of 100 km. Because the Vavilov basin formed in 3.3 Ma this gives a mean extension rate of 3 cm/y, similar to the values previously reported for the entire southern Tyrrhenian. These low extension rates and the occurrence of serpentinized mantle are typical of slow (<5 cm/y) seafloor spreading margins. Several kinematic reconstructions (Malinverno and Ryan, 1986; Faccenna et al., 2001; Malinverno, 2012) pointed to a total amount of extension in the southern Tyrrhenian region ranging between 330 and 390 km. This gives an average extension rate of 3.3–3.9 cm/y, in view of the start of the Tyrrhenian rifting 10 Ma ago.

6. Conclusions

We combined the analysis of seismic reflection profiles, borehole data, and the crustal model EuCRUST-07 (Tesauro et al., 2008), to reconstruct the 3D architecture and evolution of the triangular Vavilov backarc basin from apex to distal areas. From the results obtained we conclude that:

1. On the basis of age and sedimentary facies of the basin infill we estimate a Pliocene timing (5.1–1.8 Ma) of the rift zone formation.
2. Initial pure shear mode extension, characterized by distributed high-angle normal faulting and rift basins, was followed by simple shear mode extension, associated to detachment faults and supradetachment basins.
3. The growth of detachment faults started 4.0 Ma ago affected contemporaneously the entire basin and involves structural levels progressively deeper down to the mantle.
4. Embrittlement of the crust and through-going faults formation into the upper mantle have led to serpentization and mantle exhumation along a downward concave detachment plane in the distal region. The downward concave fault geometry can be associated to rolling hinge and isostatic adjustments.
5. The seismological Moho identified at a depth of ~10 km does not correspond to the petrological Moho, at least in the southeastern part of the basin, where the serpentinized upper mantle is exhumed at a depth ~500 m from the surface topography (ODP site 651). This interpretation implies also that continental crust in the bathyal region has been locally thinned and extended more significantly than previously estimated.
6. The opening of this triangular backarc basin occurred around an Euler pole and was geologically synchronous from the apex to the distal zones.

Acknowledgements

This study was funded by Universita'del Sannio (FRA 2015), Utrecht University, and the Netherlands Research Centre for Integrated Solid Earth Science (ISES) (ISES-2014-UU-08, ISES-2016-UUU-19). We thank IHS Inc. that furnished the Kingdom software. We are grateful to Keith Martin for the very detailed review and highly stimulating comments. Further comments provided by an anonymous reviewer are also acknowledged. We thank S. Cloetingh for his suggestions on an earlier version of the manuscript.

References

Allen, P.A., Allen, J.R., 2005. Basin analysis. Principles and Applications, 2nd edition Blackwell Publishing (549 pp).

Alvarez, W., Cocozza, T., Wezel, F.C., 1974. Fragmentation of the Alpine orogenic belt by microplate dispersal. Nature 248, 309–314.

Bally, A.W., Bernoulli, D., Davis, G.A., Montadert, L., 1981. Listric normal faults. Oceanol. Acta 26, 87–101.

Bellotti, P., Evangelista, S., Tortora, P., Valeri, P., 1997. Caratteri sedimentologici e stratigrafici dei sedimenti pliopleistocenici affioranti lungo la costa tra Tor Caldara e Anzio (Lazio centrale). Boll. Soc. Geol. Ital. 116, 79–94.

Bonatti, E., Seyler, M., Channell, J., Giraudeau, J., Mascle, G., 1990. Peridotite drilled from the Tyrrhenian Sea, ODP LEG 107. In: Kastens, K.A., Mascle, J., et al. (Eds.), 1990 Proceedings of the Ocean Drilling Program. Scientific Results 107, pp. 37–47.

Brune, S., Heine, C., Pérez-Gussinyé, M., Sobolev, S.V., 2014. Rift migration explains continental margin asymmetry and crustal hyper-extension. Nat. Commun. 5:1–9. http://dx.doi.org/10.1038/ncomms5014.

Butler, R.W.H., Tavarnelli, E., Grasso, M., 2006. Structural inheritance in mountain belts: an Alpine–Apennine perspective. J. Struct. Geol. 28, 1893–1908.

Cadoux, A., Pinti, D., Aznar, C., Chiesa, S., Gillot, P.Y., 2005. New chronological and geochemical constraints on the genesis and geologic evolution of Ponza and Palmarola Volcanic Islands (Thyrrenian Sea, Italy). Lithos 81, 121–151.

Cassinis, R., Scarascia, S., Lozej, A., 2003. The deep crustal structure of Italy and surrounding areas from seismic refraction data. A new synthesis. Boll. Soc. Geol. It. 122, 365–376.

Cavinato, G.P., De Celles, P.G., 1999. Extensional basins in the tectonically bimodal central Appennines fold-thrust belt, Italy: response to corner flow above a sub-ducting slab in retrograde motion. Geology 27, 955–958.

Channell, J.E.T., Rio, D., Sprovieri, R., Glaçon, G., 1990. Biomagnetostratigraphic correlations from Leg 107 in the Tyrrhenian Sea. In: Kastens, K.A., Mascle, J., et al. (Eds.), Proceedings of the Ocean Drilling ProgramScientific Results 107. Ocean Drilling Program, College Station, TX, pp. 669–682.

Chian, D., Louden, K.F., Minshull, T., Whitmarsh, R., 1999. Deep structure of the ocean-continent transition in the southern Iberian Abyssal Plain from seismic refraction profiles: Ocean Drilling Program (Legs 149 and 173) transect. J. Geophys. Res. 104 (B4), 7443–7462.

Christensen, N.I., 2004. Serpentinites, peridotites, and seismology. Int. Geol. Rev. 46 (9): 795–816. http://dx.doi.org/10.2747/0020-6814.46.9.795.

Christensen, N.I., Mooney, W.D., 1995. Seismic velocity structure and composition of the continental crust: a global view. J. Geophys. Res. 100 (B7), 9761–9788.

Cloetingh, S., Burov, E., Matenco, L., Beekman, F., Roure, F., Ziegler, P.A., 2013. The Moho in extensional tectonic settings: insights from thermo-mechanical models. Tectonophysics 609, 558–604.

Coney, P.J., 1987. The regional tectonic setting and possible causes of Cenozoic extension in the North American Cordigliera. In: Coward, M., Dewey, J., Hancock, P. (Eds.), Continental Extensional Tectonics. Geol. Soc. Spec. Publ 28, pp. 177–186.

Cooper, M.A., Williams, G.D. (Eds.), 1989. Inversion tectonicsGeol. Soc. Lond., Spec. Publ. 44.

Cornamusini, G., Lazzarotto, A., Merlini, S., Pascucci, V., 2002. Eocene-Miocene evolution of the north Tyrrhenian Sea. Boll. Soc. Geol. Ital. 1, 769–787.

Corti, G., Van Wijk, J., Bonini, M., Sokoutis, D., Cloetingh, S., Innocenti, F., Manetti, P., 2003. Transition from continental break-up to punctiform seafloor spreading: how fast, symmetric and magmatic. Geophys. Res. Lett. 30 (12):1604. http://dx.doi.org/10.1029/2003GL017374.

Coward, M., Dewey, J., Hancock, P. (Eds.), 1987. Continental Extensional Tectonics. Geol. Soc. Spec. Publ 28 (637 pp).

Dart, C.J., Collier, R.E.L., Gawthorp, R.L., Keller, J.V., Nichols, G., 1994. Sequence stratigraphy of (?) Pliocene–Quaternary syn-rift Gilbert type deltas, northern Peloponnesos, Greece. Mar. Pet. Geol. 11, 545–560.

De Rita, D., Funiciello, R., Pantosti, D., Salvini, F., Sposato, A., Velonà, M., 1986. Geological and structural characteristics of the Pontine islands (Italy) and implications with the evolution of the Tyrrhenian margin. Mem. Soc. Geol. Ital. 36, 55–65.

Della Vedova, B., Bellani, S., Pellis, G., Squarci, P., 2001. Deep temperatures and surface heat flow distribution. In: Vai, G.B., Martini, I.P. (Eds.), Anatomy of an Orogen: The Apennines and Adjacent Mediterranean Basins. Kluwer Academic Publishers, Dordrecht, The Netherlands, pp. 65–76.

Deschamps, F., Godard, M., Guillot, S., Hattori, K., 2013. Geochemistry of subduction zone serpentinites: a review. Lithos 178, 96–127.

Dewey, J.F., Helman, M.L., Turco, E., Hutton, D.H.W., Knott, S.D., 1989. Kinematics of the Western Mediterranean. In: Coward, M.P., Dietrich, D., Park, R.G. (Eds.), Alpine Tectonics 45. Geol. Soc. London Spec. Pub, pp. 225–283.

Espur, N., Callot, J., Roure, F., Totterdell, J.M., Struckmeyer, H.I.M., Vially, R., 2012. Transition from symmetry to asymmetry during continental rifting: an example from the Bight Basin–Terre Adélie (Australian and Antarctic conjugate margins). Terra Nova 24:167–180. http://dx.doi.org/10.1111/j.1365-3121.2011.01055.x.

Faccenna, C., Funiciello, R., Bruni, A., Mattei, M., Sagnotti, L., 1994. Evolution of a transfer-related basin: the Ardea basin (Latium, Central Italy). Basin Res. 6, 31–46.

Faccenna, C., Davy, P., Brun, J.P., Funiciello, R., Giardini, D., Mattei, M., Nalpas, T., 1996. The dynamic of backarc basins: an experimental approach to the opening of the Tyrrhenian Sea. Geophys. J. Int. 126, 781–795.

Faccenna, C., Becker, T.W., Lucente, F.P., Jolivet, L., 2001. History of subduction and back-arc extension in the Central Mediterranean. Geophys. J. Int. 145, 809–820.

Florio, G., Fedi, M., Cella, F., 2011. Insights on the spreading of the Tyrrhenian Sea from the magnetic anomaly pattern. Terra Nova 23:127–133. http://dx.doi.org/10.1111/j.1365-3121.2011.00992.x.

Friedman, S.J., Burbank, D.W., 1995. Rift basins and supradetachment basins: Intracontinental extensional end-members. Basin Res. 7, 109–127.

Gawthorpe, R.L., Leeder, M.R., 2000. Tectono-sedimentary evolution of active extensional basins. Basin Res. 12, 195–218.

Hamilton, W., 1987. Crustal extension in the Basin and Range Province, southwestern United States. In: Coward, M.P., Dewey, J.F., Hancock, P.L. (Eds.), Continental Extensional Tectonics 28. Geol. Soc. London Spec. Pub, pp. 155–176.

Harris, L.B., Koy, H.K., Fossen, H., 2002. Mechanisms for folding of high-grade rocks in extensional tectonic settings. Earth-Sci. Rev. 59, 163–210.

Hauser, F., O'Reilly, B.M., Jacob, A.W.B., Shannon, P.M., Makris, J., Vogt, U., 1995. The crustal structure of the Rockall trough: differential stretching without underplating. J. Geophys. Res. 100:4097–4116. http://dx.doi.org/10.1029/94jb02879.

Hsu, et al., 1978. Site 373: Tyrrhenian Basin. Deep Sea Drilling Project Volume XLII Part 1, pp. 151–174.

Iannace, P., Milia, A., Torrente, M.M., 2013. 4D geologic evolution in the Gaeta Baysedimentary infill (Eastern Tyrrhenian Sea). GeoActa 12, 25–36 (Bologna).

Kapp, P., Taylor, M., Stokling, D., Ding, L., 2008. Development of active low-angle normal fault systems during orogenic collapse: insight from Tibet. Geology 36:7–10. http://dx.doi.org/10.1130/G24054A.1.

Kastens, K., Mascle, J., 1990. The geological evolution of the Tyrrhenian Sea: an introduction to the scientific results of ODP Leg 107. In: Kastens, K.A., Mascle, J., et al. (Eds.), Proc. ODP, SciResults 107. Ocean Drilling Program, College Station, TX, pp. 3–26.

Kastens, K.A., et al., 1987. Proceedings ODP, Initial. Reports 107. Ocean Drilling Program, College Station, TX (999 pp).

Keen, C.E., 1987. Some important consequences of lithospheric extension. In: Coward, M.P., Dewey, J.F., Hancock, P.L. (Eds.), Continental Extensional Tectonics. Geological Society, London, Special Publications 28, pp. 67–73.

Lavier, L.L., Manatschal, G., 2006. A mechanism to thin the continental lithosphere at magma-poor margins. Nature 440:324–328. http://dx.doi.org/10.1038/nature04608.

Lister, G.S., Etheridge, M.A., Symonds, P.A., 1986. Application of the detachment fault model to the formation of passive continental margins. Geology 14, 246–250.

Lombardi, L., 1968. Il pozzo Fogliano nei pressi di Latina e la palegeografia dell'area. Boll. Soc. Geol. Ital. 87, 13–18.

Malatesta, A., Zarlenga, F., 1985. Il Quaternario di Pomezia (Roma) e la sua fauna marina. Boll. Soc. Geol. Ital. 104, 503–514.

Malatesta, A., Zarlenga, F., 1986. Evoluzione paleogeografico-strutturale Plio-Pleistocenica del basso bacino romano a nord e a sud del Tevere. Mem. Soc. Geol. It. 35, 75–85.

Malinverno, A., Ryan, W.B.F., 1986. Extension in the Tyrrhenian Sea and shortening in the Apennines as result of arc migration driven by sinking of the lithosphere. Tectonics 5, 227–245.

Malinverno, A., 2012. Evolution of the Tyrrhenian Sea-Calabrian Arc system: The past and the present. Rend. Online Soc. Geol. It. 21, 11–15.

Manatschal, G., 2004. New models for evolution of magma-poor rifted margins based on a review of data and concepts from West Iberia and the Alps. Int. J. Earth Sci. 93, 432–466.

Marani, M., Trua, T., 2002. Thermal constriction and slab tearing at the origin of a superinflated spreading ridge: Marsili volcano (Tyrrhenian Sea). J. Geophys. Res. 107 (B9):2188. http://dx.doi.org/10.1029/2001jb000285.

Marani, M., Taviani, M., Trincardi, F., Argnani, A., Borsetti, A., Zitellini, N., 1986. Pleistocene progradation and post-glacial events of the NE Tyrrhenian continental shelf between the Tiber delta and Capo Circeo. Mem. Soc. Geol. Ital. 36, 67–89.

Marani, M., Gamberi, G., Bortoluzzi, G., Carrarra, G., Ligi, M., Penitenti, D., 2004. Seafloor morphology of the Tyrrhenian Sea. Scale 1:1,000,000. Included to: Mem. Descr. Carta Geol. Ital., LXIV. Rome.

Mariani, M., Prato, R., 1988. I bacini neogenici costieri del margine tirrenico: approccio sismico-stratigrafico. Mem. Soc. Geol. Ital. 41, 519–531.

Martin, A.K., 1984. Propagating rifts: crustal extension during continental rifting. Tectonics 3, 611–617.

Martin, A.K., 2006. Oppositely directed pairs of propagating rifts in backarc basins: double saloon door seafloor spreading during subduction rollback. Tectonics 25, TC3008. http://dx.doi.org/10.1029/2005TC001885.

Mascle, J., Rehault, J.-P., 1990. A revised seismic stratigraphy of the Tyrrhenian Sea: implications for the basin evolution. In: Kastens, K.A., Mascle, J., et al. (Eds.), Proceedings of the Ocean Drilling Program, Scientific Results, 107. Ocean Drilling Program, College Station, TX, pp. 617–634.

Masini, E., Manatschal, G., Mohn, G., Unternehr, P., 2012. Anatomy and tectono-sedimentary evolution of a rift-related detachment system: the example of the Err detachment (Central Alps, SE Switzerland). Geol. Soc. Am. Bull. 124, 1535–1551.

McClay, K.R., Ellis, P.G., 1987. Analogue models of extensional fault geometries. In: Coward, M., Dewey, J., Hancock, P. (Eds.), Continental Extensional Tectonics. Geol. Soc. Spec. Publ 28, pp. 109–125.

McKenzie, D.P., 1978. Some remarks on the development of sedimentary basins. Earth Planet. Sci. Lett. 40, 25–32.

Milia, A., Torrente, M.M., 2014. Early-stage rifting of the southern Tyrrhenian region: the Calabria-Sardinia breakup. J. Geodyn. 81:17–29. http://dx.doi.org/10.1016/j.jog.2014.06.001.

Milia, A., Torrente, M.M., 2015a. Tectono-stratigraphic signature of a rapid multistage subsiding rift basin in the Tyrrhenian-Apennine hinge zone (Italy): a possible interaction of upper plate with subducting slab. J. Geodyn. 86:42–60. http://dx.doi.org/10.1016/j.jog.2015.02.005.

Milia, A., Torrente, M.M., 2015b. Rift and supradetachment basins during extension: insight from Tyrrhenian rift. J. Geol. Soc. 72:5–8. http://dx.doi.org/10.1144/jgs2014-046.

Milia, A., Torrente, M.M., Massa, B., Iannace, P., 2013. Progressive changes in rifting directions in the Campania margin (Italy): new constrains for the Tyrrhenian Sea opening. Glob. Planet. Chang. 109:3–17. http://dx.doi.org/10.1016/j.gloplacha.2013.07.003.

Mitchum, R.M., Vail, P.R., Sangree, J.B., 1977. Seismic stratigraphy and global changes of sea level, part 6: stratigraphic interpretation of seismic reflection patterns in depositional sequences. In: Payton, C.E. (Ed.), Seismic Stratigraphy – Application to Hydrocarbon Exploration. Am. Ass. Petr. Geol. Mem 26, pp. 117–133.
Mongelli, F., Loddo, M., Calcagnile, G., 1975. Some observations of the Apennines gravity field. Earth Planet. Sci. Lett. 24, 385–393.
Nicolich, R., 1989. Crustal structure from seismic studies in the frame of the European Geotraverse (Southern segment) and CROP project. In: Boriani, A., Bonafede, M., Piccardo, G.B., Vai, G.B. (Eds.), The Lithosphere in Italy. Advances in Earth Science Research. Atti Convegni dei Lincei 80, pp. 41–61.
Nicolosi, I., Speranza, F., Chiappini, M., 2006. Ultrafast oceanic spreading of the Marsili Basin, southern Tyrrhenian Sea: evidence from magnetic anomaly analysis. Geology 34, 717–720.
O'Reilly, B.M., Hauser, F., Ravaut, C., Shannon, P.M., Readman, P.W., 2006. Crustal thinning, mantle exhumation and serpentinization in the Porcupine Basin, offshore Ireland: evidence from wide-angle seismic data. J. Geol. Soc. 163:775–787. http://dx.doi.org/10.1144/0016-76492005-079.
Panza, G.F., 1984. Structure of the lithosphere–asthenosphere system in the Mediterranean region. Ann. Geophys. 2, 137–138.
Panza, G., Calcagnile, G., 1979/1980. The upper mantle structure in Balearic and Tyrrhenian bathyal plains and the Messinian salinity crisis. Palaeogeogr. Palaeoclimatol. Palaeoecol. 29, 3–14.
Pascucci, V., 2002. Tyrrhenian Sea extension north of the Elba Island between Corsica and western Tuscany (Italy). Boll. Soc. Geol. Ital. 1, 819–828.
Patacca, E., Sartori, R., Scandone, P., 1990. Tyrrhenian basin and Apenninic arcs: kinematic relations since late Tortonian times. Mem. Soc. Geol. Ital. 45, 425–451.
Péron-Pinvidic, G., Manatschal, G., Minshull, T.A., Sawyer, D.S., 2007. Tectonosedimentary evolution of the deep Iberia-Newfoundland margins: evidence for a complex breakup history. Tectonics 26, TC2011. http://dx.doi.org/10.1029/2006TC001970.
Platt, J.P., Behr, W.M., Cooper, F.J., 2015. Metamorphic core complexes: windows into the mechanics and rheology of the crust. J. Geol. Soc. 172:9–27. http://dx.doi.org/10.1144/jgs2014-036.
Prada, M., Sallares, V., Ranero, C.R., Vendrell, M.G., Grevemeyer, I., Zitellini, N., de Franco, R., 2014. The complex 3-D transition from continental crust to backarc magmatism and exhumed mantle in the Central Tyrrhenian basin. Geophys. J. Int. 203 (2015): 63–78. http://dx.doi.org/10.1093/gji/ggv271.
Reston, T.J., 2009. The structure, evolution and symmetry of the magma-poor rifted margins of the North and Central Atlantic: a synthesis. Tectonophysics 468, 6–27.
Reston, T.J., Pérez-Gussinyé, M., 2007. Lithospheric extension from rifting to continental breakup at magma-poor margins: rheology, serpentinisation and symmetry. Int J. Earth Sci. (Geol Rundsch) 96:1033–1046. http://dx.doi.org/10.1007/s00531-006-0161-z.
Robin, C., Colantoni, P., Genessaux, M., Rehault, J.P., 1987. Vavilov seamount: a midly alkaline Quaternary volcano in the Tyrrhenian basin. Mar. Geol. 78, 125–136.
Rosenbaum, G., Lister, G.S., 2004. Neogene and Quaternary rollback evolution of the Tyrrhenian Sea, the Apennines, and the Sicilian Maghrebides. Tectonics 23, TC1013. http://dx.doi.org/10.1029/2003TC001518.
Roure, F., Casero, P., Addoum, B., 2012. Alpine inversion of the North African margin and delamination of its continental lithosphere. Tectonics 31. http://dx.doi.org/10.1029/2011TC002989 (TCXXX).
Ruppel, C., 1995. Extensional processes in continental lithosphere. J. Geophys. Res. 100, 187–215.
Saintot, A., Stephenson, R., Brem, A., Stovba, S., Privalov, V., 2003. Paleostress field reconstruction and revised tectonic history of the Donbas fold-and-thrust belt (Ukraine and Russia). Tectonics 22, 1059.
Sartori, R., 1990. The main results of ODP Leg 107 in the frame of neogene to recent geology of Perityrrhenian areas. In: Kastens, K.A., Mascle, J., et al. (Eds.), Proceedings of the Ocean Drilling ProgramScientific Results 107. Ocean Drilling Program, College Station, TX, pp. 715–730.
Sartori, R., 2003. The Tyrrhenian back-arc basin and subduction of the Ionian lithosphere. Episodes 26 (3), 217–221.
Sartori, R., 2005. Bedrock geology of the Tyrrhenian Sea insight on Alpine paleogeography and magmatic evolution of the basin. In: Finetti, I.R. (Ed.), CROP Project: Deep Seismic Exploration of the Central Mediterranean and Italy. Elsevier, Amsterdam, pp. 69–80.
Sartori, R., Torelli, L., Zitellini, N., Carrara, G., Magaldi, M., Mussoni, P., 2004. Crustal features along a W-E Tyrrhenian transect from Sardinia to Campania margins (Central Mediterranean). Tectonophysics 383, 171–192.
Sauter, D., et al., 2013. Continuous exhumation of mantle-derived rocks at the southwest Indian Ridge for 11 million years. Nat. Geosci. 6:314–320. http://dx.doi.org/10.1038/NGEO1771.
Savelli, C., Lipparini, E., 1978. K/Ar age determinations on basalt rocks from hole 373 A. Deep Sea Drilling Project Volume XLII Part 1, pp. 537–539.
Schellart, W.P., Jessell, M.W., Lister, G.S., 2003. Asymmetric deformation in the backarc region of the Kuril arc, northwest Pacific: new insights from analogue modeling. Tectonics 22:1047. http://dx.doi.org/10.1029/2002TC001473.
Scrocca, D., Doglioni, C., Innocenti, F., 2003a. Constraints for an interpretation of the Italian geodynamics: a review. Mem. Descr. Carta Geol. Ital. 62, 15–46.
Scrocca, D., Doglioni, C., Innocenti, F., Manetti, P., Mazzotti, A., Bertelli, L., Burbi, L., D'Offizi, S., 2003b. Crop atlas seismic reflection profiles on the Italian crust. Mem. Descritt. Carta Geol. Ital. 62, 1–193 (36 plates enclosed).
Serri, G., 1990. Neogene–quaternary magmatism of the Tyrrhenian region: characterization of magma sources and geodynamic implications. Mem. Soc. Geol. Ital. 41, 219–242.
Smit, J., Brun, J.-P., Cloetingh, S., Ben-Avraham, Z., 2010. The rift-like structure and asymmetry of the Dead Sea Fault. Earth Planet. Sci. Lett. 290, 74–82.
Snedden, J.W., Liu, C.L., 2010. A Compilation of Phanerozoic Sea-level Change, Coastal Onlaps and Recommended Sequence Designations. Search and Discovery, Article# 40594.
Sokoutis, D., Corti, G., Bonini, M., Brun, J.P., Cloetingh, S., Mauduit, T., Manetti, P., 2007. Modelling the extension of heterogeneous hot lithosphere. Tectonophysics 444, 63–79.
Spadini, G., Cloetingh, S., Bertotti, G., 1995. Thermo-mechanical modelling of the Tyrrhenian Sea: lithosphere necking and kinematics of rifting. Tectonics 14, 629–644.
Stephenson, R., Yegorova, T., Brunet, M.-F., Stovba, S., Wilson, M., Starostenko, V., Saintot, A., Kusznir, N., 2006. Late Palaeozoic intra- and pericratonic basins on the East European Craton and its margins. In: Gee, D.G., Stephenson, R.A. (Eds.), European Lithosphere Dynamics 32. Geol. Soc. of London, Mem., pp. 463–479.
Taylor, B. (Ed.), 1995. Backarc Basins. Tectonics and Magmatism. Plenum Press (524pp).
Tesauro, M., Kaban, M.K., Cloetingh, S.A.P.L., 2008. EuCRUST-07: a new reference model for the European crust. Geophys. Res. Lett. 35, L05313. http://dx.doi.org/10.1029/2007GL032244.
Torrente, M.M., Milia, A., Bellucci, F., Rolandi, G., 2010. Extensional tectonics in the Campania Volcanic Zone (eastern Tyrrhenian Sea, Italy): new insights into relationship between faulting and ignimbrite eruptions. Ital. J. Geosci. 129:297–315. http://dx.doi.org/10.3301/IJG.2010.07.
ViDEPI, 2009. Progetto Visibilità Dati Esplorazione Petrolifera in Italia. © 2009–2010 Ministero dello Sviluppo Economico UNMIG, Soci-età Geologica Italiana Assomineraria (last accessed on 25.11.11, http://unmig.sviluppoeconomico.gov.it/videpi/).
Violanti, D., 2012. Pliocene Mediterranean foraminiferal biostratigraphy: a synthesis and application to the paleoenvironmental evolution of northwestern Italy. In: Elitok, Ö. (Ed.), Stratigraphic Analysis of Layered Deposits, pp. 123–160 (ISBN: 978-953-51-0578-7, InTech).
Washington, H.S., 1906. The Roman Comagmatic Region. vol. 57. Carnegie Institute, Washington, pp. 1–199.
Wernicke, B.P., 1985. Uniform-sense normal simple shear of the continental lithosphere. Can. J. Earth Sci. 22, 108–124.
Wernicke, B.P., Axen, G.J., 1988. On the role of isostasy on the evolution of normal fault systems. Geology 16, 848–851.
Whitmarsh, R.B., Manatschal, G., Minshull, T.A., 2001. Evolution of magma-poor continental margins from rifting to seafloor spreading. Nature 413, 150–154.
Ziegler, P.A., 1992. Plate tectonics, plate moving mechanisms and rifting. Tectonophysics 215, 9–34.
Ziegler, P.A., Cloetingh, S., 2004. Dynamic processes controlling evolution of rifted basins. Earth Sci. Rev. 64, 1–50.